QIBA Profile:
Diffusion-Weighted Magnetic Resonance Imaging (DWI)

Stage: A. Initial Draft

Notation in this Template		
Template Element	**Appears as**	**Instructions**
Boilerplate text	Plain black text	Don't change. Should appear in all profiles.
Example text	Plain grey text	Provides an example of content and wording appropriate to that location. Rewrite it to your needs and change the text color back to Automatic (which will make it black).
Placeholder	<text in angle brackets>	Replace text and <> with your text. Use Find/Replace for ones that appear frequently.
Guidance	Comment with "GUIDANCE" at the top.	Delete it when you've followed it and don't need it anymore.

Table of Contents

Change Log:

This table is a best-effort of the authors to summarize significant changes to the Profile.

Date	Sections Affected	Summary of Change
2015.10.10	All	Major cleanup based on comments resolved in the Process Cmte. Also had to remove a few hundred extraneous paragraph styles.
2015.10.21	All	Approved by Process Cmte
2015.11.04	2 (Claims) 3 (Requirements)	Incorporating the more refined form of the claim language and referenced a separate claim template. Added Voxel Noise requirement to show example of the linkage between the requirement and the assessment procedure.
2015.12.16		Minor changes to remove reference to "qualitative" measurements, fix reference to guidance and clean some formatting.
2016.01.06	1, 3.8.1	Rewording to avoid the term "accuracy".
2016.11.21	2	Removed polygonal brain ROI area reference (not literature-supported)
2017.01.18	All	Endnote library of references, prostate added, reconciled ToC with actual content, fixed formatting, cleaned up most comments and highlights, ready for PDF review

Open Issues:

The following issues are provided here to capture associated discussion, to focus the attention of reviewers on topics needing feedback, and to track them so they are ultimately resolved. In particular, comments on these issues are highly encouraged during the Public Comment stage.

Q. Who to include in Appendix B **A.** RSNA staff has provided current roster, this is an issue that can be addressed in Google Docs while PDF is reviewing, with a final review at the BC level prior to handoff to MR CC.
Q. Comments in Prostate Section **A.** As the most recently edited organ section, we ask PDF readers to examine the claims and justifications prior to moving up to the MR CC level.
Q. Include images of relevant artifacts for Image QA section 3.8 **A.** While PDF is reviewing, the TF members will look for appropriate examples of DWI artifacts in brain, liver and prostate to include in Appendix

Closed Issues:

The following issues have been considered closed by the biomarker committee. They are provided here to forestall discussion of issues that have already been raised and resolved, and to provide a record of the rationale behind the resolution.

Q. Which organs have sufficient reproducibility literature for inclusion in the longitudinal claim statement? A. Organs for inclusion are brain, liver, and prostate. The following organs were considered, but have been excluded for the time being due to lack of sufficient literature (test-retest data from a total of ~35 subjects, either from a single publication or in total from multiple manuscripts) support: Bone Breast Kidney Lymphoma Pancreas Head and neck Lung Whole Body
Q. How much of the Subject Handling subsection (3.1) is applicable to DWI? A. Text has been adjusted according to standard clinical practice, subject to public review
Q. Should organ-specific protocols be changed to the profile template's table format, or left as-is? **A.** Protocols were adapted for the three organs discussed in the first DWI profile.
Q. Can references be better formatted? A. Now using EndNote Library in Word, not sure how this will translate to Google Docs.
Q. How to make conformance section conform? **A.** Old Conformance section moved mostly to Appendices, current structure reflects profile template from Process Committee
Q. What DICOM parameters should be specified in section 3.2.2? **A.** In public tags, vendors should provide: *b*-value; diffusion gradient direction (3-vector) or "isotropic"; sequence class (single spin-echo monopolar; single spin-echo bipolar; double spin-echo bipolar; stimulated echo); **This was addressed, section is now 3.6**

1. Executive Summary

The goal of a QIBA Profile is to help achieve a useful level of performance for a given biomarker. The **Claim** (Section 2) describes the biomarker performance. The **Activities** (Section 3) contribute to generating the biomarker. Requirements are placed on the **Actors** that participate in those activities as necessary to achieve the Claim. **Assessment Procedures** (Section 4) for evaluating specific requirements are defined as needed to ensure acceptable performance.

Diffusion-Weighted Imaging (DWI) and the Apparent Diffusion Coefficient (ADC) are being used clinically as qualitative indicators of disease presence, progression or response to treatment [1-29] . Use of ADC as a robust quantitative biomarker with finite confidence intervals places additional requirements on Acquisition Devices and Protocols, Technologists, Radiologists, Scientists, Reconstruction Software and Image Analysis Tools [30-37]. All of these are considered **Actors** involved in **Activities** of Subject Handling, Image Data Acquisition, Reconstruction, Quality Assurance (QA) and Analysis. The requirements addressed in this Profile are focused on achieving ADC values within a known (ideally negligible) systematic bias range and avoiding unnecessary technical measurement variability [34, 36, 37].

DISCLAIMER: Technical performance of the MRI system can be assessed using a phantom having known diffusion properties, such as the QIBA DWI phantom. The clinical performance target is to achieve a 95% confidence interval for measurement of ADC with a variable precision depending on the organ being imaged and assuming adequate technical performance requirements are met. While in vivo DWI/ADC measurements have been performed throughout the human body, this Profile focused on three organ systems, namely brain, liver, and prostate as having high clinical utilization of ADC with a sufficient level of statistical evidence to support the Profile Claims derived from the current (as of March 2017) peer-reviewed literature. In due time, new DWI technologies with proven greater performance levels, as well as more organ systems will be incorporated in future Profiles.

Three levels of compliance for the current DWI profile specifications are defined as:

ACCEPTABLE: Failing to meet this specification will result in data that is likely unacceptable for the intended use of this profile.

TARGET: Meeting this specification is achievable with reasonable effort and adequate equipment and is expected to provide better results than meeting the ACCEPTABLE specification.

IDEAL: Meeting this specification may require extra effort or non-standard hardware or software, but is expected to provide better results than meeting the TARGET.

This document is intended to help a variety of users: clinicians using this biomarker to aid patient management; imaging staff generating this biomarker; MRI system architects developing related products; purchasers of such products; and investigators designing clinical trials utilizing quantitative diffusion-based imaging endpoints.

Note that this document only states requirements to achieve the claim, not requirements that pertain to clinical standard of care." Conforming to this Profile is secondary to proper patient care.

2. Clinical Context and Claims

Clinical Context

The goal of this profile is to facilitate appropriate use of quantitative diffusion weighted imaging (DWI) to gain insight into the microstructure and composition of lesions in humans using precise quantitative measurements of the apparent diffusion coefficient (ADC) for robust tissue characterization and longitudinal tumor monitoring. The premise for its use is that therapy-induced cellular necrosis should pre-date macroscopic lesion size change, thereby motivating exploration of ADC as a response biomarker [3, 5, 6, 13, 14, 16, 18, 19, 22, 26, 27, 38, 39]. Within days to weeks after initiation of effective cytotoxic therapy, tumor necrosis occurs, with a loss of cell membrane integrity and an increase of the extracellular space typically resulting in a relative increase in ADC. During the following weeks to months, the tumor may show shrinkage with a resorption of the free extracellular fluid and fibrotic conversion leading to a decrease of the ADC, although tumor recurrence can also result in reduced ADC [21, 40, 41].

The objective of this Profile is to provide prerequisite knowledge of the expected level of variance in ADC measurement unrelated to treatment, in order to properly interpret observed change in ADC following treatment [30, 34, 36].

This QIBA DWI Profile makes Claims about the confidence with which ADC values and changes in a lesion can be measured under a set of defined image acquisition, processing, and analysis conditions. It also provides specifications that may be adopted by users and equipment developers to meet targeted levels of clinical performance in identified settings. The intended audience of this document includes healthcare professionals and all other stakeholders invested in the use of quantitative diffusion biomarkers for treatment response and monitoring, including but not limited to:

- Radiologists, technologists, and physicists designing protocols for ADC measurement
- Radiologists, technologists, physicists, and administrators at healthcare institutions considering specifications for procuring new MR equipment
- Technical staff of software and device manufacturers who create products for this purpose
- Biopharmaceutical companies
- Clinicians engaged in therapy response monitoring
- Clinical trialists
- Radiologists and other health care providers making quantitative measurements on ADC maps
- Oncologists, urologists, neurologists, other clinicians, regulators, professional societies, and others making decisions based on quantitative diffusion image measurements
- Radiologists, health care providers, administrators and government officials developing and implementing policies for brain, liver, and prostate cancer treatment and monitoring

Conformance to this Profile <u>by all relevant staff and equipment</u> supports the following claim(s):

Claim 1a: A measured change in the ADC of a brain lesion of 11% or larger indicates that a true change has occurred with 95% confidence.

Claim 2a: A measured change in the ADC of a liver lesion of 26% or larger indicates that a true change has occurred with 95% confidence.

Claim 3a: A measured change in the ADC of a prostate lesion of 47% or larger indicates that a true change has occurred with 95% confidence.

Claim 1b: A 95% CI for the true change in ADC of a brain lesion is given below, where Y_1 and Y_2 are the ADC measurements at the two time points:

$$(Y_2 - Y_1) \pm 1.96 \times \sqrt{(Y_1 \times 0.040)^2 + (Y_2 \times 0.040)^2}.$$

Claim 2b: A 95% CI for the true change in ADC of a liver lesion is given below, where Y_1 and Y_2 are the ADC measurements at the two time points:

$$(Y_2 - Y_1) \pm 1.96 \times \sqrt{(Y_1 \times 0.094)^2 + (Y_2 \times 0.094)^2}.$$

Claim 3b: A 95% CI for the true change in ADC of a prostate lesion is given below, where Y_1 and Y_2 are the ADC measurements at the two time points:

$$(Y_2 - Y_1) \pm 1.96 \times \sqrt{(Y_1 \times 0.17)^2 + (Y_2 \times 0.17)^2}.$$

These claims hold when:

- The same imaging methods on the same scanner and the same analysis methods are used at two separate time points where the interval between measurements is intended to represent the evolution of the tissue over the interval of interest (such as pre-therapy versus post initiation of therapy).
- Conspicuity of lesion boundary is adequate to localize the lesion for definition on a region-of-interest [27] at both time points.

Discussion

- These claims are based on estimates of the within-subject coefficient of variation (wCV) for ROIs drawn in the brain, liver and prostate. For estimating the critical % change, the % Repeatability Coefficient (%RC) is used: 2.77 × wCV × 100%, or %RC = 11% for brain, 26% for liver, 47% for prostate. Specifically, it is assumed that the wCV is 4% for brain, 9% for liver, and 17% for prostate. The claim assumes that the wCV is constant for tissue regions in the specified size, the signal-to-noise ratio (SNR) of the tissue region on the *b*=0 image is at least 50, and that the measured ADC is linear (slope=1) with respect to the true ADC value over the range 0.25×10^{-3} mm^2/s to 2.5×10^{-3} mm^2/s.
- For the brain, estimates are from Bonekamp 2007, Pfefferbaum 2003 (mean ADC in an anatomical region or polygonal ROI), and Paldino 2009 [42-44]; for the liver, estimates are from Miquel 2012, Braithwaite 2009 (mean ADC in an ROI between 1-4 cm^2) [45-48]; for the prostate, estimates are from Litjens 2012 and Gibbs 2007 (Table 1 of the manuscript, mean ADC is from an ROI ranging from 120 to 320 mm^2, with little impact on repeatability) [49-52].

In tumors, changes in ADC can reflect variations in cellularity, as inferred by local tissue water mobility, e.g., a reduction or increase of the extracellular space, although the level of measured change must be interpreted relative to the Repeatability Coefficient before considered as a true change [1, 30, 34, 37, 53-55]. Other biological processes may also lead to changes in ADC, e.g., stroke.

While the Profile Claims have been informed by a review of the literature and expert consensus, the Claims have not yet been fully substantiated by studies that strictly conform to the specifications given here. The expectation is that during field test, data on the actual field performance will be collected and any appropriate changes made to the claim or the details of the Profile. At that point, this caveat may be removed or re-stated.

3. Profile Activities

The Profile is documented in terms of "Actors" performing "Activities". Equipment, software, staff or sites may claim conformance to this Profile as one or more of the "Actors" in the following table.

Conformant Actors shall support the listed Activities by conforming to all requirements in the referenced Section.

Table 1: Actors and Required Activities

Actor	Activity	Section
Acquisition Device / Physicist / Field Engineer	Pre-delivery & Installation	3.1. & 3.2.
	Periodic QA	3.3.
	Image Data Acquisition	3.6.
MR Technologist / Physicist / Scientist	Subject Selection & Handling	3.4. & 3.5.
	Image Data Acquisition	3.6.
	Image Data Reconstruction	3.7.
Radiologist Image Analyst / Physicist / Scientist	Image QA	3.8.
	Image Distribution	3.9.
	Image Analysis & Interpretation	3.10. & 3.11.
Reconstruction Software	Image Data Reconstruction	3.7.
Image Analysis Tool	Image Analysis	3.10.

The requirements in this Profile do not codify a Standard of Care; they only provide guidance intended to achieve the stated Claim. Failing to conform to a "shall" statement in this Profile is a protocol deviation. Although deviations invalidate the Profile Claim, such deviations may be reasonable and unavoidable and the radiologist or supervising physician is expected to do so when required by the best interest of the patient or research subject. Handling protocol deviations for specific trials/studies is at full discretion of the study sponsors and other responsible parties.

The sequencing of Activities specified in this DWI Profile is shown in Figure 1:

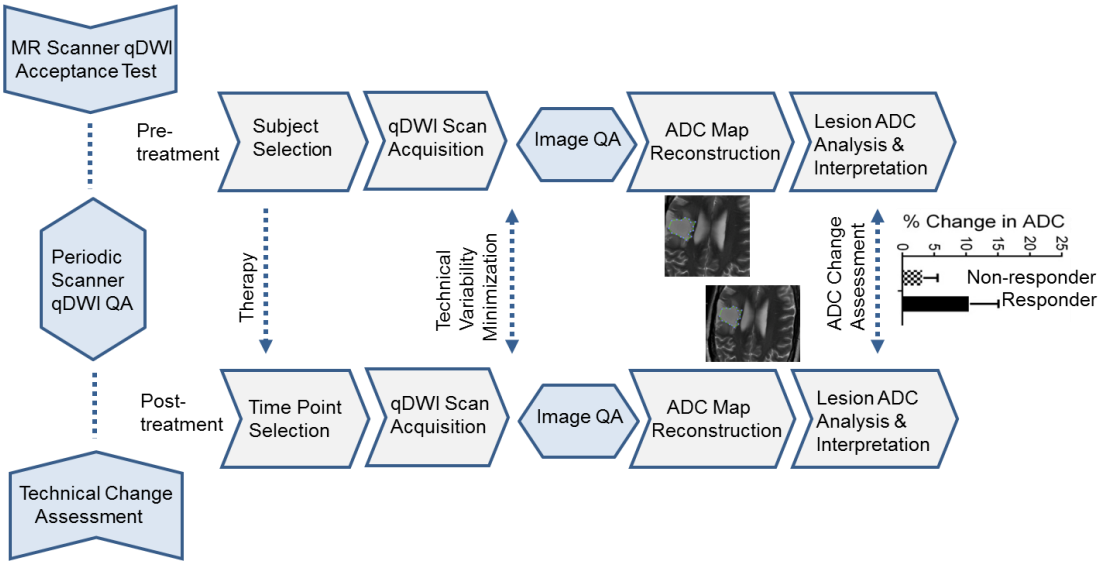

Figure 1: Diffusion-Weighted MRI for Treatment Response Assessment - Activity Sequence

3.1. Pre-delivery

This activity describes calibrations, phantom imaging, performance assessments or validations prior to delivery of equipment to a site (e.g. performed at the factory) that are necessary to reliably meet the Profile Claim.

3.1.1 Discussion

Current clinical MR scanners with DWI capabilities are adequate. No additional specific pre-delivery activities are required for this Profile.

3.2. Installation

This activity describes calibrations, phantom imaging, performance assessments or validations that are part of commissioning acceptance testing and follow installation of equipment at the site that are necessary to reliably meet the Profile Claim.

3.2.1 Discussion

Installation needs to be done by a trained field service engineer as per manufacturers' specifications and supervised by a local MR physicist. No additional specific installation activities are required by this Profile.

3.3. Periodic QA

This activity describes phantom imaging, performance assessments or validations performed periodically at the site, but not directly associated with a specific subject, that are necessary to reliably meet the Profile Claim.

3.3.1 Discussion

Quality assurance procedures shall be consistent with those generally accepted for routine clinical imaging. The imaging device should have periodic performance assessment using methods and procedures defined by the MRI vendor, or other nationally/internationally recognized bodies such as

American Association of Physicists in Medicine (AAPM) [56], American College of Radiology (ACR), The Joint Commission or corresponding organizations in other countries. Preventive maintenance at appropriate regular intervals shall be conducted and documented by a qualified service engineer as recommended by the scanner manufacturer. Additional, DWI-specific QA procedures to ensure baseline scanner performance with minimal technical variability are described in Section 4 and Appendix D and E, and can be utilized as needed [21, 57].

3.3.2 SPECIFICATION

Parameter	Actor	Requirement
Accreditation of site/system	Physicist / Scientist	Shall be performed by a Qualified MRI Medical Physicist or MRI scientist as defined by appropriate accrediting bodies
System performance metrics	Field Engineer / Physicist / Scientist	System shall perform within vendor-established performance benchmark ranges for the given scanner model
Periodic DWI QC	Physicist / Scientist	Shall perform periodic system QC that includes assessment of ADC bias, random error, linearity, DWI SNR, DWI image artifacts, *b*-value dependence and spatial uniformity

3.4. Subject Selection

This activity describes criteria and procedures related to the selection of appropriate imaging subjects that are necessary to reliably meet the Profile Claim.

3.4.1 DISCUSSION

All subjects considered safe for clinical MRI may be considered for a DWI study. Implants and devices categorized with status "MR Unsafe" are considered an absolute contraindication [58-61]. Implants and devices having status "MR Safe" or "MR Conditional" shall be evaluated per local MRI safety review procedures to assess relative risk status. Despite having an acceptable risk status, metal-containing implants and devices near the tissue/organ/lesion of interest may introduce artifact and may not be suitable for DWI. Contraindications unrelated to implants should be considered as well. These include but are not limited to: 1st trimester pregnancy, claustrophobia, age and subject's ability to cooperate [62-65].

For specific study/trial, subject scan timing should be appropriately synchronized with the assayed subject condition (e.g., clinical state or therapeutic phase) per study design.

3.5. Subject Handling

This activity describes details of handling imaging subjects that are necessary to reliably meet the Profile Claim.

3.5.1 DISCUSSION

DWI patients should be prepared according to local standard of care (e.g. safety screening and removal of all metal objects and electronic devices) [58-60, 66]; otherwise no additional specific patient preparation procedures are required. Patients should wear appropriate attire (site-provided scrubs are preferred) and

be comfortably positioned to minimize patient motion and stress, which might affect the imaging results. At present, there is no consensus concerning all patient preparation issues.

To reduce motion artifact from bowel peristalsis during prostate imaging, the use of an antispasmodic agent may be beneficial in some patients. However, in many others it is not necessary, and the incremental cost and potential for adverse drug reactions should be taken into consideration. The presence of stool in the rectum may interfere with placement of an endorectal coil. If an ERC is not used, the presence of air and/or stool in the rectum may induce artifactual distortion that can compromise DWI quality. Thus, some type of minimal preparation enema administered by the patient in the hours prior to the exam maybe beneficial. However, an enema may also promote peristalsis, resulting in increased motion related artifacts in some instances. The patient should evacuate the rectum, if possible, just prior to the MRI exam.

Parameter	Actor	Requirement
Patient Positioning	Technologist	Serial study of each individual patient shall be performed on the same scanner using the same receiver coil and same positioning procedure (e.g. always head-first or always feet-first)

3.6. Image Data Acquisition

This activity describes details of the data acquisition process that are necessary to reliably meet the Profile Claim. It may also include calibrations, performance assessments or validations during acquisition that are necessary to reliably meet the Profile Claim.

3.6.1 Discussion

Tables in section 3.6.2 contain key specifications expressed using generic terminology. The specifications are consistent with publications supporting Profile Claims and consensus recommendations for brain [31, 42-44, 67], liver [21, 28, 45-48, 55] and prostate [49-52, 54]. (Appendix D tabulates a standardized DWI phantom scanning protocol in vendor-specific terms that may be useful to harmonize patient DWI protocol across platforms [68-71].) Some parameters include a numerical range, and some requirements include qualifiers “acceptable” (base level to meet the claim), “target” (typical or default level to meet the claim), and “ideal” (expected higher performance available on some systems). Reduction of respiratory artifact in the liver requires either short breath-hold (un-averaged, <25 sec), or long (3-5 min) respiratory-synchronization, or free breathing with high signal averaging. The gain in image quality with high signal averaging favors use of non-breath-hold abdominal DWI. Section 4 and Appendix E describe DWI-specific (phantom-based) assessment procedures to ensure sufficient control of technical variability in DWI image acquisition to achieve the current Profile claims [68-75]. New techniques, such as simultaneous multi-slice or multi-band MRI, are becoming commercially available and could be advantageous for DWI [76-79]. However, these are not yet considered “standard” on most clinical systems and therefore are not specified below.

3.6.2 Specification

The same acquisition methods repeated on the same scanner using parameter settings tabulated below are necessary to reliably meet the Profile Claim. DWI scan protocols shall be built by the MR technologist and/or MR physicist/scientist, clearly labeled and stored on the MRI system for recall in repeatable serial scan of patients. Version control of edits to the protocol should be tracked with prior versions archived.

BRAIN

Parameter	Actor	Requirement	DICOM Tag
Field Strength	MR technologist /Physicist/ Scientist	1.5 or 3T	[0018, 0087]
Acquisition sequence		Diffusion-weighted Single-Shot Echo Planar Imaging (SS-EPI)	[0018, 0020]
Receive Coil type		Ideal: 32 channel head array coil	[0018, 1250]
		Target: 8-32 channel head array coil	
		Acceptable: 8 channel head array coil	
Lipid suppression		On	
Number of *b*-values		Ideal: ≥3 (including one *b*=0)	
		Acceptable/Target: 2 (including *b*=0)	
Minimum highest *b*-value strength		Target/Ideal: *b*=1000 s/mm^2	[0018, 9087]
		Acceptable: *b*=850-999 s/mm^2	
Diffusion directions		Target/Ideal: ≥3-orthogonal, combined gradient channels	[0018, 9075]
		Acceptable: ≥3-orthogonal, single gradient channels	[0018, 9089]
Slice thickness		Ideal: ≤4 mm	[0018, 0050]
		Target: 4-5 mm	
		Acceptable: 5mm	
Gap thickness		Target/Ideal: 0-1 mm Acceptable: 1-2 mm	[0018, 0088]
Field-of-view		Ideal/Target/Acceptable: 220-240 mm FOV along both axes	[0018, 1100]
Acquisition matrix		Target/Ideal: (160-256) x (160-256), or 1.5-1 mm in-plane resolution	[0018, 1310]
		Acceptable: 128 x 128, or 1.7 mm in-plane resolution	
Plane orientation		Transversal-axial	[0020, 0037]
Phase-encode/ frequency-encode direction		Anterior-Posterior / Right-Left	[0018, 1312]
Number of averages		Ideal/Target: ≥ 2	[0018, 0083]
		Acceptable:1	

In-plane parallel imaging acceleration factor		Ideal: 2-3 Acceptable/Target: 2	[0018, 9069]
TR		Ideal: > 5000 ms Acceptable/Target: 3000-5000 ms	[0018, 0080]
TE		Ideal: <60ms	[0018, 0081]
		Target: minimum TE	
		Acceptable: <120 ms	
Receiver Bandwidth		Ideal/Target: maximum possible in frequency encoding direction (minimum echo spacing)	[0018, 0095]
		Acceptable:>1000 Hz/voxel	

LIVER

Parameter	Actor	Requirement	DICOM Tag
Field Strength	MR technologist / Physicist / Scientist	1.5 or 3 T	[0018, 0087]
Acquisition sequence		Diffusion-weighted Single-Shot Echo Planar Imaging (SS-EPI)	[0018, 0020]
Receive Coil type		Ideal: >16 channel torso array coil Target: >6-16 channel torso array coil Acceptable: 6 channel torso array coil	[0018, 1250]
Lipid suppression		On	
Number of *b*-values		Ideal: ≥3 (including one *b*<50-100 s/mm^2)	
		Acceptable/Target: 2 (including one *b*<50-100s/mm^2)	
Minimum highest *b*-value strength		Target/Ideal: *b*=600-800 s/mm^2	[0018, 9087]
		Acceptable: 500 s/mm^2	
Diffusion directions		Target/Ideal: 3-orthogonal, combined gradient channels Acceptable: 3-orthogonal, single gradient channels	[0018, 9075] [0018, 9089]
Slice thickness		Ideal: <5 mm	[0018, 0050]
		Target: 5-7 mm	
		Acceptable: 7-9 mm	
Gap thickness		Ideal: 0 mm	[0018, 0088]
		Target:1 mm	
		Acceptable:>1-2 mm	
Field-of-view		Ideal/Target/Acceptable: 300-450 mm	[0018, 1100]
Acquisition matrix		Target/Ideal: (160-196) x (160-192), or 2.5-2	

		mm in-plane Acceptable: 128 x 128, or 3-2.6 mm in-plane resolution	[0018, 1310]
Plane orientation		Transversal-axial	[0020, 0037]
Phase-encode/ frequency-encode direction		Anterior-Posterior / Right-Left	[0018, 1312]
Number of averages		Ideal: > 4	[0018, 0083]
		Target: 4	
		Acceptable:2-3	
Parallel imaging factor		Ideal: 2-3	[0018, 9069]
		Target/Acceptable: 2	
TR		Ideal/Target/Acceptable> 2000 ms	[0018, 0080]
TE		Ideal: < 60 ms	[0018, 0081]
		Target: minimum TE	
		Acceptable: < 110 ms	
Receiver Bandwidth		Ideal/Target: maximum possible in frequency encoding direction (minimum echo spacing)	[0018, 0095]
		Acceptable: > 1000 Hz/voxel	

PROSTATE

Parameter	Actor	Requirement	DICOM Tag
Field Strength	MR technologist / Physicist / Scientist	3 T	[0018, 0087]
Acquisition sequence		Diffusion-weighted Single-Shot Echo Planar Imaging (SS-EPI)	[0018,0020]
Receive Coil type		Ideal: >8 channel torso array coil Target: >8 channel torso array coil Acceptable: pelvic phased array coil/endorectal coil; body array coil	[0018,1250]
Lipid suppression		On	
Number of *b*-values		Ideal: ≥3 (including one *b*<50-100 s/mm^2)	
		Acceptable/Target: 2 (including one *b*<50-100s/mm^2)	
Minimum highest *b*-value strength		Ideal: *b*=1000-1500 s/mm^2	[0018, 9087]
		Target/Acceptable: 500-1000 s/mm^2	
Diffusion directions		Target/Ideal: 3-orthogonal, combined	

		gradient channels Acceptable: 3-orthogonal, single gradient channels	[0018, 9075] [0018, 9089]
Slice thickness		Ideal: <3 mm Target: 3-4 mm Acceptable: 4-5 mm	[0018, 0050]
Gap thickness		Ideal: 0 mm Target/Acceptable: 1 mm	[0018, 0088]
Field-of-view		Ideal/Target/Acceptable: 240-260 mm	[0018, 1100]
Acquisition matrix		Target/Ideal/Acceptable: (224-128) x (224-128), or 1-2 mm in-plane	[0018, 1310]
Plane orientation		Transversal-axial	[0020, 0037]
Phase-encode/ frequency-encode direction		Anterior-Posterior / Right-Left	[0018, 1312]
Number of averages		Ideal: > 4 Target: 4 Acceptable:2-4	[0018, 0083]
Parallel imaging factor		Ideal /Target/Acceptable: 2	[0018, 9069]
TR		Ideal/Target/Acceptable> 2000 ms	[0018, 0080]
TE		Ideal: < 60 ms Target: minimum TE Acceptable: < 90 ms	[0018, 0081]
Receiver Bandwidth		Ideal/Target: maximum possible in frequency encoding direction (minimum echo spacing) Acceptable: > 1000 Hz/voxel	[0018, 0095]

3.7. Image Data Reconstruction

This activity describes criteria and procedures related to producing images from the acquired data that are necessary to reliably meet the Profile Claim.

3.7.1 Discussion

At a minimum, three-orthogonal directional DWI are acquired and reconstructed individually for each imaged slice, then combined into a directionally-independent (i.e. isotropic or trace) DWI [80, 81]. Diffusion weighted images may be interpolated to an image matrix greater than the acquired matrix. Trace DWI (e.g. geometric average of 3-orthogonal directional DWI at same *b*-value) shall be automatically generated on the scanner and retained for each non-zero *b*-value, whereas retention of directional DWI is optional. ADC maps are typically generated on the scanner using a mono-exponential model trace DWI vs *b*-value. Alternatively, full DWI sets (directional plus trace, or trace alone) at all *b*-values can be provided for off-line ADC map generation (via mono-exponential model) on an independent workstation or thin-client distributed application.

Eddy currents and/or subject motion may create spatial misalignment or distortion between the individual directional DWI, and across *b*-values [82-84]. Direct combination of misaligned directional DWI will lead to spatial blur in trace DWI and subsequent artifact in ADC maps [82-84]. Spatial registration of directional DWI and/or trace DWI across all *b*-values may be performed on the scanner or off-line to reduce blur and improve quality of trace DWI and ADC maps.

Perfusion is known to affect diffusion measurement (a positive bias) particularly in highly vascular tissues (e.g. kidney and liver) [85-90]. ADC values derived from DWI spanning low *b*-value (i.e. $b<50 s/mm^2$) and modest high *b*-value (i.e. $b<500 s/mm^2$) increase perfusion bias. For diffusion measurement in liver, ADC maps may be reconstructed from DWI spanning 50-100s/mm^2 up to 800-900s/mm^2 to mitigate perfusion bias while maintaining adequate sensitivity to diffusion contrast and SNR. The *b*-value range used for ADC map generation shall be recorded and reported. Perfusion bias in brain DWI is considered small and typically ignored. There is a small deviation from monoexponential decay (pseudodiffusion) at low *b*-values in prostate [91].

3.7.2 Specification

Parameter	Actor	Requirement
Trace DWI and ADC map generation	MR technologist / Physicist / Scientist	Procedural steps for image reconstruction/ADC map generation shall be held constant for all subjects and time points including: image interpolation; image registration prior to combination into trace DWI and across *b*-values; selection of *b*-values and fit algorithm to estimate ADC. ADC shall be calculated using the mono-exponential model of DWI signal decay with increasing *b*-value.

3.8. Image QA

This activity describes criteria and evaluations of the images that are necessary to reliably meet the Profile Claim.

3.8.1 Discussion

At the time of image acquisition and review, quality of DWI data shall be checked for the following issues. Poor quality due to sources below may be grounds to reject individual datasets.

- Low SNR – Diffusion weighting inherently reduces signal, although signal must remain adequately above the noise floor to properly estimate ADC [92-94]. Low SNR at high *b*-values can bias ADC estimates. Visualization of anatomical features in tissues of interest at all *b*-values is acceptable evidence that SNR is adequate for ADC measurement.

- Ghost/parallel imaging artifacts – Discrete ghosts from extraneous signal sources along phase-encode direction can obscure tissue of interest leading to unpredictable ADC values [83, 95-98].

- Severe spatial distortion – Some level of spatial distortion is inherent to SS-EPI, although distortion can be severe near high susceptibility gradients in tissues or metallic objects; or due to poor magnet homogeneity [83, 97]. Severe distortion can alter apparent size/shape/volume of tissues of interest thereby confound ROI definition, as well as adversely affect ADC values. Co-registration to high-resolution (non-EPI) T_2-weighted image volume may reduce these distortions.

- Eddy currents – Distinct eddy currents amplified by strong diffusion pulses on different gradient channels lead to spatial misalignment across DWI directions and *b*-values, and manifest as spatial blur on trace DWI and erroneous ADC values, particularly at the edges of anatomical features [83, 99]. Distortion correction and image registration to $b = 0$ image prior to calculation of trace DWI and ADC maps may reduce these errors.

- Fat suppression – Lipid exhibits extremely low diffusion, with fat spatially shifted on SS-EPI from its true source (by several cm along the phase-encode direction) due to chemical shift [100-104]. Of note, scanner frequency drifting due to the heating from high duty cycle diffusion gradients could cause unsatisfactory fat suppression in the later frames of a diffusion acquisition, if only chemical shift saturation technique is used for fat suppression. In such case, alternative or additional fat suppression techniques, e.g. gradient reversal, could help to mitigate residual fat signal. Superposition of unsuppressed fat signal onto tissue of interest can invalidate ADC assessment there by partial volume averaging.

- Motion artifacts — While SS-EPI is effective at freezing most bulk motion, variability of motion over DWI directions and *b*-values contribute to blur and erroneous signal attenuation. Motion artifact is anticipated to be low in brain DWI for most subjects, although cardiac-induced pulsation can confound ADC measurement in/near ventricles and large vessels and in the brainstem. Respiratory and cardiac motion artifacts are more problematic in the liver, particularly the left-lobe and superior right lobe [12, 28, 97, 105, 106]. Quiet steady breathing or respiratory synchronization and additional signal averaging are used to mitigate motion artifact in abdominal DWI. Residual motion artifact can be recognized as inconsistent location of anatomical targets across *b*-values and DWI directions and/or spatial modulation unrelated to anatomical features on DWI/ADC maps. Inspection of DWI/ADC on orthogonal multiplanar reformat images aids detection of this artifact.

3.8.2 SPECIFICATION

Parameter	Actor	Requirement
ADC	Radiologist / MR technologist / Physicist / Scientist	Shall confirm DWI and ADC maps conform to adequate quality specifically considering points listed above (3.8.1).

3.9. Image Distribution

This activity describes criteria and procedures related to distributing, transferring and archiving images and metadata that are necessary to reliably meet the Profile Claim.

3.9.1 DISCUSSION

Images are distributed via network using Digital Imaging and Communications in Medicine (DICOM) transfer protocol as per standard local practice. At a minimum, trace DWI at each acquired *b*-value must be archived in the local picture archiving and communication system (PACS). Additionally, individual direction DWI and ADC maps (if generated on the scanner) should be archived. DICOM tags essential for downstream review and diffusion analysis must be maintained including, pixel intensity scaling [107], *b*-value, and DWI directionality vs trace. DWI DICOM tags that store this information currently vary among vendors. DICOM Parametric Map object [108] should be considered for storage of ADC maps, as it provides unambiguous encoding of the quantity, units, b-values used and derivation method used for ADC calculation [109]. The use of DICOM Parametric Map can facilitate interoperable and standardized description of the DWI analysis results. It is noted that this object type is a recent introduction to the DICOM standard and is not widely adopted among the vendors [108, 109].

3.9.2 SPECIFICATION

Parameter	Actor	Requirement
Trace DWI	MR technologist / Physicist / Scientist	All trace DWI at each acquired *b*-value shall be stored in local PACS and distributed to image analysis workstation(s)
ADC maps		ADC maps generated on the MRI scanner shall be stored in local PACS and distributed to image analysis workstation(s). *b*-values used for ADC map generation shall be recorded.
Directional DWI		If directional DWI were generated on the MRI scanner in DICOM format, these shall be stored in local PACS and distributed to image analysis workstation(s).

3.10. Image Analysis

This activity describes criteria and procedures related to producing quantitative measurements from the images that are necessary to reliably meet the Profile Claim.

General considerations

In addition to initial Image QA (section 3.8), the radiologist / image analyst should confirm MR exams are complete with all anatomical and DWI series, as well as screen for artifacts on DWI/ADC. Severe artifact

may lead to incorrect ADC calculation and should be excluded from ROIs placed on tissues of interest. ADC maps shall be generated using mono-exponential model of signal attenuation vs *b*-value over the range specified in section 3.6.2. ADC maps used for image analysis must be "equivalent" to ADC maps generated on the MRI system. That is, all software elements along the image handling/network chain must appropriately deal with potential DICOM scaling of DWI and ADC pixel values [107], otherwise quantitative content is lost. The difference(s) in mean ADC within replicate ROIs defined on the scanner and analysis workstation(s) should be less than the ROI standard deviation of the ADC. If ADC maps used for analysis are generated offline, correct DICOM pixel scaling should be confirmed using a phantom having absolute known ADC value (see Appendix D and E) or a DWI DRO (https://goo.gl/yYPG0W).

3.10.1 Discussion: ROI definition in DWI imaging

The measurements should be similar to those performed in ordinary clinical conditions. Level and range of slices with tissue/tumor of interest should be reasonably matched each time the measurements are performed. The use of ancillary MR images (e.g. T_1-weighted, T_2-weighted, post-gadolinium) can aid lesion identification prior to ROI placement [21, 57, 67]. Tissue or lesion ADC quantification requires manual placement of an ROI in two or three-dimensions. When performing ROI placement, the user must decide which sequences (DWI, ADC maps, T_2-weighted, T_1-weighted with gadolinium, etc.) will be used to ***guide*** selection tissue to be assayed, but the actual placement of the ROIs shall be on the diffusion images.

Procedural steps to create and extract quantities from ROIs varies among software packages. At times, histogram analysis of whole tumor ROIs may be preferable to allow for distinction between predominantly solid and heterogeneous cystic/necrotic lesions. Analysis steps, derived metrics and analysis software package shall be held constant for all subjects and serial time points.

Recommendations for ROI placement are organ-specific.

3.10.1.1 Brain

ROIs should be manually placed on axial images where the tissues of interest are adequately conspicuous on the DWI and/or ADC maps, or identifiable guided by ancillary MR images. The size of the ROI should be chosen by the radiologist, though should be defined on relatively homogenous regions and matched to select the same lesion/tissue assayed on prior time points. Selected ROI size should be sufficient to represent the targeted ADC statistics. Avoid contamination within the ROI from tissues such as CSF or that may have high iron content, such as acute or chronic hemorrhagic areas that have anomalous ADC values. The brain may also contain areas of large necrotic cysts and surgical cavities - these areas should be avoided.

3.10.1.2 Liver

For liver parenchyma evaluation, ROIs should be large enough to avoid ADC values being unduly influenced by random image noise and/or under-sampled regional heterogeneity. ROI placement should avoid large vessels or extraneous anomalous ADC tissue unrelated to target tissue of interest such as cysts or hemangiomas. Comparison of DWI at *b*=0 having high SNR revealing both vessels and focal lesions, to moderately low *b* (< 100 s/mm^2) where vessels are suppressed can be useful to localize lesions. It is also important when assessing the ADC of liver parenchyma to avoid the lateral segment of the left lobe, as this area is subject to pulsatile effects from the heart, leading to bias in high ADC values.

For liver lesion evaluation, the image that best reveals the lesion at high conspicuity is recommended. In most cases, the low *b*-value image will provide the best visualization of lesion location and margins.

However, low *b*-value images alone will not allow the reader to distinguish between benign and malignant lesions, and inspection of higher *b*-value images and/or the ADC map is recommended.

For large liver lesions, special consideration must be given to lesion heterogeneity. Large malignant lesions of the liver may contain areas of central necrosis or cystic degeneration. Avoidance of these areas is recommended so that one is limiting the quantitative assay to areas of solid tissue/tumor. However, while avoidance of cystic or necrotic areas is desirable, tumor effects that are marked by developing necrosis may be underestimated if one ignores cystic areas post treatment.

3.10.1.3 PROSTATE

ROIs should be manually placed on axial images by the radiologist where the tissues of interest are adequately conspicuous on the DWI and/or ADC maps, or identifiable guided by ancillary MR images.

3.10.2 SPECIFICATION

Parameter	Actor	Requirement
ROI Determination	Radiologist / Image Analyst / Scientist	Shall segment the ROI consistently across time points using the same software / analysis package
Image Display	Image Analysis Tool	Acceptable / Target: Software shall allow operator-defined ROI analysis of DWI/ADC aided by inspection of ancillary MR contrasts Ideal: Above plus multi view-port display where DWI/ADC and ancillary MR contrasts from the same scan date are displayed side-by-side and geometrically linked per DICOM (e.g cursor; cross-hair; ROI; automatically replicated in all view-ports); images from different scan date(s) can be displayed side-by-side, though not necessarily geometrically linked; and ROIs/VOIs may include multiple noncontiguous areas on one slice and/or over multiple slices
ADC statistics	Image Analysis Tool	Acceptable/Target: Shall allow display and retention of ROI statistics in patient DICOM database. Statistics shall include: ADC mean, standard deviation, and ROI/VOI area/volume Ideal: Additional statistics for ADC maximum, minimum, explicit inclusion vs exclusion of “NaNs” or zero-valued pixels in statistics, ADC pixel histogram, and retention of the ROI/VOI as a DICOM segmentation object

3.11. Image Interpretation

This activity describes criteria and procedures related to clinically interpreting the measurements and images that are necessary to reliably meet the Profile Claim.

3.11.1 DISCUSSION

Low ADC values suggest cellular dense tissue and potentially solid/viable tumor as opposed to elevated

ADC values in tumor necrosis and cystic spaces. The use of specific interpretation of ADC values will depend on the clinical application, e.g., taking into account spontaneous tumor necrosis versus tumor necrosis after effective therapy. Schema and properties of tissues to assay by ADC should be addressed during the design phase of each study. For example, therapies targeted to induce cytotoxic change in solid viable tumor [3, 19, 22, 38, 40] are candidate for ADC monitoring by ROI segmentation guided by traditional MR indicators of solid viable tissue, namely: relatively hyperintense on high *b*-value DWI, low ADC, and perfused on dynamic contrast-enhanced MRI. The anticipated timescale of ***early*** therapeutic response and/or tumor progression must be considered in study design of MRI scan dates for application of ADC as a prognostic marker.

4. Assessment Procedures

To conform to this Profile, participating staff, software and equipment (**Actors**) shall support each activity assigned to them in Table 1.

To support an activity, the **Actor** shall conform to the requirements (indicated by "shall" language) listed in the specifications table of the activity subsection in Section 3.

Although most of the requirements described in Section 3 can be assessed for conformance by direct observation, some of the baseline quantitative DWI performance-oriented requirements cannot, in which case the requirement will reference an assessment procedure in a subsection here in Section 4.

Formal claims of conformance by the organization responsible for an Actor shall be in the form of a published QIBA Conformance Statement. Vendors publishing a QIBA Conformance Statement shall provide a set of "Model-Specific Parameters" (as shown in Appendix D) describing how their product was configured to achieve conformance for quantitative DWI acquisition and analysis. Vendors shall also provide access or describe the characteristics of the test set used for conformance testing.

4.1. Assessment Procedure: MRI Equipment Specifications and Performance

Conformance with this Profile requires adherence of MRI equipment to U.S. federal regulations [110] or analogous regulations outside of the U.S., MRI equipment performance standards outlined by the American Association of Physicists in Medicine [56] and/or by the American College of Radiology* as well as quality control benchmarks established by the scanner manufacturer for the specific model. These assessment procedures include a technical performance evaluation of the MRI scanner by a qualified medical physicist or MRI scientist at least annually. Evaluated parameters include: magnetic field uniformity, patient-handling equipment, gradient and RF subsystems safety, calibration and performance checks. Periodic MR quality control must monitor image uniformity, contrast, spatial resolution, signal-to-noise and artifacts using specific test objects and procedures (e.g., ACR phantom and QA procedure). In addition, preventive maintenance at appropriate regular intervals must be conducted and documented by a qualified service engineer.

Gradient subsystems are *explicitly* calibrated to properly encode 3D space, and are *implicitly* calibrated to also encode diffusion. Performance procedures indicated above assess spatial encoding quality, although diffusion weighting performance requires additional tests detailed in Appendix E. Key quantitative DWI performance metrics include: ADC bias at magnet isocenter, random error within ROI (precision), SNR at each *b*-value, ADC dependence on *b*-value and ADC spatial dependence. To conform to this Profile, system performance benchmarks for these metrics are provided in Appendix E to ensure negligible contribution of technical errors to above defined confidence intervals measured for tissue. These benchmarks reflect the baseline MRI equipment performance in clinical and clinical trial settings which produced the data used to support the Claims of this Profile. To establish tighter confidence bounds for ADC metrics, additional technical assessment procedures may be introduced according to specific clinical trial protocol.

*http://www.acr.org/~/media/ACR No Index/Documents/QC Manual/2015_MR_QCManual_Book.pdf.

4.2. Assessment Procedure: Technologist

Radiologic technologists shall fulfill the qualifications required by the ACR MRI Accreditation Program** or analogous non-U.S. accreditation programs for non-U.S. facilities. These include certification by the

American Registry of Radiologic Technologists (ARRT) or analogous non-U.S. certifying organization, appropriate licensing, documented training and experience in performing MRI, and compliance with certifying and licensing organization continuing education requirements. The technologist shall be capable of building, performing, and saving QA and DWI acquisition protocols for their specific system to be consistent with this Profile. The technologist must be capable to perform all image processing steps to create ADC maps on the scanner, and to recognize when automatic "in-line" ADC maps are defective (e.g. noise threshold set too high causing artefactual null ADC zones in tissues).
**http://www.acraccreditation.org/~/media/ACRAccreditation/Documents/MRI/Requirements.pdf?la=en

4.3. Assessment Procedure: Radiologists

Radiologists shall fulfill the qualifications required by the ACR MRI Accreditation Program*** or analogous non-U.S. accreditation programs for non-U.S. facilities. These include certification by the American Board of Radiology or analogous non-U.S. certifying organization; appropriate licensing; documented oversight, interpretation, and reporting of the required ABR minimum number of MRI examinations; and compliance with ABR and licensing board continuing education requirements. Diffusion MRI does not specifically require additional certification of the radiologist.

***http://www.acraccreditation.org/~/media/ACRAccreditation/Documents/MRI/Requirements.pdf?la=en

4.4. Assessment Procedure: Image Analyst / Physicist / Scientist

In clinical practice, it is expected that the radiologist interpreting the examination often will be the image analyst. In some clinical practice situations, and in the clinical research setting, the image analyst may be a non-radiologist professional such as a medical physicist, biomedical engineer, MRI scientist or 3D lab technician. While there are currently no specific certification guidelines for image analysts, a non-radiologist performing diffusion analysis shall be trained in technical aspects of DWI including: understanding key acquisition principles of diffusion weighting and directionality and diffusion test procedures (Appendix E); procedures to confirm that diffusion-related DICOM metadata content is maintained along the network chain from scanner to PACS and analysis workstation. The analyst must be expert in use of the image analysis software environment, including ADC map generation from DWI (if not generated on the scanner), and ADC map reduction to statistics with ROI/VOI location(s) retained. The analyst shall undergo documented training by a radiologist having qualifications conforming to the requirements of this profile in terms of anatomical location and image contrast(s) used to select measurement target. The level of training should be appropriate for the setting and the purpose of the measurements, and may include instruction in topics such as directional and isotropic DWI and ADC map reconstruction and processing; normative ADC values for select tissues; and recognition of image artifacts.

4.5. Assessment Procedure: Image Analysis Software

Often ADC maps are generated on the MRI system and distributed to the analysis workstation along with source DWI and other available anatomical series. The image analyst / scientist must confirm ADC values generated and measured on the scanner (e.g. mean ADC over a 1cm circular ROI) are equivalent to

replicate ROI values defined on scanner-generated ADC maps using intended analysis software. The level of "equivalence" should be well within the ROI standard deviation. Discrepancy comparable to or greater than the standard deviation suggests erroneous scaling of the ADC map by the image analysis software, possibly due to incorrect or missing DICOM information. Any such discrepancy must be resolved before proceeding with statistical analysis for profile compliance. Absolute image scaling and units of analysis software-generated ADC maps must be available and stored in public DICOM tags such as RealWorldValueMapping [0040,9096], RescaleIntercept [0028,1052], RescaleSlope [0028,1053] and RescaleType [0028,1054] such that ADC map values are properly interpretable (e.g. "A true diffusion coefficient of $1.1x10^{-3}$ mm^2/s is represented by an ADC map pixel/ROI value on the analysis workstation as 1100."). The use of the DICOM Parametric Map object [108, 109] can eliminate these discrepancies, as it allows for storage of floating point voxel values. It also provides unambiguous encoding of the quantity, units, b-values used and derivation method used for ADC calculation [109]. Image analysis software vendors should consider the use of this object for storage of ADC maps.

When the image analysis software is used to generate ADC maps from source DWI, the software must use a mono exponential model of DWI signal versus *b*-value. The DWI used to derive ADC maps shall be "directionally-independent" (i.e. isotropic or trace DWI). If used for ADC map generation, image analysis software must be able to extract *b*-value and diffusion axis direction content from the DICOM header to appropriately derive ADC maps. In the event directionally-independent DWIs are not available, at least three-orthogonal axes DWI must be provided at each non-zero *b*-value so that DWI traces at each *b*-value are calculable for subsequent ADC map generation within the analysis software. The numerical software conformance and signal-to-noise sensitivity (bias and range linearity with respect to ground-truth ADC values) can be tested over the range of *b*-values and tissue-like ADC using the DWI digital reference object [56], available on the QIDW (https://goo.gl/yYPG0W).

References

1. Baehring, J.M. and R.K. Fulbright, *Diffusion-weighted MRI in neuro-oncology.* CNS Oncol, 2012. **1**(2): p. 155-67.
2. Barboriak, D.P., *Imaging of brain tumors with diffusion-weighted and diffusion tensor MR imaging.* Magn Reson Imaging Clin N Am, 2003. **11**(3): p. 379-401.
3. Chenevert, T.L., et al., *Diffusion MRI: a new strategy for assessment of cancer therapeutic efficacy.* Mol Imaging, 2002. **1**(4): p. 336-43.
4. deSouza, N.M., A. Rockall, and S. Freeman, *Functional MR Imaging in Gynecologic Cancer.* Magn Reson Imaging Clin N Am, 2016. **24**(1): p. 205-22.
5. Galban, S., et al., *Diffusion-weighted MRI for assessment of early cancer treatment response.* Curr Pharm Biotechnol, 2010. **11**(6): p. 701-8.
6. Gao, X., et al., *Magnetic resonance imaging in assessment of treatment response of gamma knife for brain tumors.* Chin Med J (Engl), 2011. **124**(12): p. 1906-10.
7. Garcia-Figueiras, R., A.R. Padhani, and S. Baleato-Gonzalez, *Therapy Monitoring with Functional and Molecular MR Imaging.* Magn Reson Imaging Clin N Am, 2016. **24**(1): p. 261-88.
8. Higano, S., et al., *Malignant astrocytic tumors: clinical importance of apparent diffusion coefficient in prediction of grade and prognosis.* Radiology, 2006. **241**(3): p. 839-46.
9. Kang, Y., et al., *Gliomas: Histogram analysis of apparent diffusion coefficient maps with standard- or high-b-value diffusion-weighted MR imaging--correlation with tumor grade.* Radiology, 2011. **261**(3): p. 882-90.
10. Kim, M. and H.S. Kim, *Emerging Techniques in Brain Tumor Imaging: What Radiologists Need to Know.* Korean J Radiol, 2016. **17**(5): p. 598-619.
11. Kim, S., et al., *Diffusion-weighted magnetic resonance imaging for predicting and detecting early response to chemoradiation therapy of squamous cell carcinomas of the head and neck.* Clin Cancer Res, 2009. **15**(3): p. 986-94.
12. Koh, D.M., et al., *Body Diffusion-weighted MR Imaging in Oncology: Imaging at 3 T.* Magn Reson Imaging Clin N Am, 2016. **24**(1): p. 31-44.
13. Lupo, J.M. and S.J. Nelson, *Advanced magnetic resonance imaging methods for planning and monitoring radiation therapy in patients with high-grade glioma.* Semin Radiat Oncol, 2014. **24**(4): p. 248-58.
14. Maier, S.E., Y. Sun, and R.V. Mulkern, *Diffusion imaging of brain tumors.* NMR Biomed, 2010. **23**(7): p. 849-64.
15. Murakami, R., et al., *Grading astrocytic tumors by using apparent diffusion coefficient parameters: superiority of a one- versus two-parameter pilot method.* Radiology, 2009. **251**(3): p. 838-45.
16. Nelson, S.J., *Assessment of therapeutic response and treatment planning for brain tumors using metabolic and physiological MRI.* NMR Biomed, 2011. **24**(6): p. 734-49.
17. Padhani, A.R., *Diffusion magnetic resonance imaging in cancer patient management.* Semin Radiat Oncol, 2011. **21**(2): p. 119-40.
18. Padhani, A.R. and A. Gogbashian, *Bony metastases: assessing response to therapy with whole-body diffusion MRI.* Cancer Imaging, 2011. **11 Spec No A**: p. S129-45.
19. Padhani, A.R. and D.M. Koh, *Diffusion MR imaging for monitoring of treatment response.* Magn Reson Imaging Clin N Am, 2011. **19**(1): p. 181-209.
20. Padhani, A.R., D.M. Koh, and D.J. Collins, *Whole-body diffusion-weighted MR imaging in cancer: current status and research directions.* Radiology, 2011. **261**(3): p. 700-18.

21. Padhani, A.R., et al., *Diffusion-weighted magnetic resonance imaging as a cancer biomarker: consensus and recommendations.* Neoplasia, 2009. **11**(2): p. 102-25.
22. Patterson, D.M., A.R. Padhani, and D.J. Collins, *Technology insight: water diffusion MRI--a potential new biomarker of response to cancer therapy.* Nat Clin Pract Oncol, 2008. **5**(4): p. 220-33.
23. Pope, W.B., et al., *Recurrent glioblastoma multiforme: ADC histogram analysis predicts response to bevacizumab treatment.* Radiology, 2009. **252**(1): p. 182-9.
24. Provenzale, J.M., S. Mukundan, and D.P. Barboriak, *Diffusion-weighted and perfusion MR imaging for brain tumor characterization and assessment of treatment response.* Radiology, 2006. **239**(3): p. 632-49.
25. Rosenkrantz, A.B., et al., *Body diffusion kurtosis imaging: Basic principles, applications, and considerations for clinical practice.* J Magn Reson Imaging, 2015. **42**(5): p. 1190-202.
26. Schmainda, K.M., *Diffusion-weighted MRI as a biomarker for treatment response in glioma.* CNS Oncol, 2012. **1**(2): p. 169-80.
27. Shiroishi, M.S., J.L. Boxerman, and W.B. Pope, *Physiologic MRI for assessment of response to therapy and prognosis in glioblastoma.* Neuro Oncol, 2016. **18**(4): p. 467-78.
28. Taouli, B. and D.M. Koh, *Diffusion-weighted MR imaging of the liver.* Radiology, 2010. **254**(1): p. 47-66.
29. Yamasaki, F., et al., *Apparent diffusion coefficient of human brain tumors at MR imaging.* Radiology, 2005. **235**(3): p. 985-91.
30. Barnhart, H.X. and D.P. Barboriak, *Applications of the repeatability of quantitative imaging biomarkers: a review of statistical analysis of repeat data sets.* Transl Oncol, 2009. **2**(4): p. 231-5.
31. Goldmacher, G.V., et al., *Standardized Brain Tumor Imaging Protocol for Clinical Trials.* AJNR Am J Neuroradiol, 2015. **36**(10): p. E65-6.
32. Jackson, E.F., et al., *Magnetic resonance assessment of response to therapy: tumor change measurement, truth data and error sources.* Transl Oncol, 2009. **2**(4): p. 211-5.
33. Meyer, C.R., et al., *Quantitative imaging to assess tumor response to therapy: common themes of measurement, truth data, and error sources.* Transl Oncol, 2009. **2**(4): p. 198-210.
34. Obuchowski, N.A., et al., *Statistical Issues in Testing Conformance with the Quantitative Imaging Biomarker Alliance (QIBA) Profile Claims.* Acad Radiol, 2016. **23**(4): p. 496-506.
35. Obuchowski, N.A., et al., *Quantitative imaging biomarkers: a review of statistical methods for computer algorithm comparisons.* Stat Methods Med Res, 2015. **24**(1): p. 68-106.
36. Raunig, D.L., et al., *Quantitative imaging biomarkers: a review of statistical methods for technical performance assessment.* Stat Methods Med Res, 2015. **24**(1): p. 27-67.
37. Sullivan, D.C., et al., *Metrology Standards for Quantitative Imaging Biomarkers.* Radiology, 2015. **277**(3): p. 813-25.
38. Li, S.P. and A.R. Padhani, *Tumor response assessments with diffusion and perfusion MRI.* J Magn Reson Imaging, 2012. **35**(4): p. 745-63.
39. O'Connor, J.P., et al., *Imaging biomarker roadmap for cancer studies.* Nat Rev Clin Oncol, 2016.
40. Chenevert, T.L., P.C. Sundgren, and B.D. Ross, *Diffusion imaging: insight to cell status and cytoarchitecture.* Neuroimaging Clin N Am, 2006. **16**(4): p. 619-32, viii-ix.
41. Ross, B.D., et al., *Evaluation of cancer therapy using diffusion magnetic resonance imaging.* Mol Cancer Ther, 2003. **2**(6): p. 581-7.
42. Bonekamp, D., et al., *Diffusion tensor imaging in children and adolescents: reproducibility, hemispheric, and age-related differences.* Neuroimage, 2007. **34**(2): p. 733-42.
43. Paldino, M.J., et al., *Repeatability of quantitative parameters derived from diffusion tensor*

imaging in patients with glioblastoma multiforme. J Magn Reson Imaging, 2009. **29**(5): p. 1199-205.
44. Pfefferbaum, A., E. Adalsteinsson, and E.V. Sullivan, *Replicability of diffusion tensor imaging measurements of fractional anisotropy and trace in brain.* J Magn Reson Imaging, 2003. **18**(4): p. 427-33.
45. Braithwaite, A.C., et al., *Short- and midterm reproducibility of apparent diffusion coefficient measurements at 3.0-T diffusion-weighted imaging of the abdomen.* Radiology, 2009. **250**(2): p. 459-65.
46. Deckers, F., et al., *Apparent diffusion coefficient measurements as very early predictive markers of response to chemotherapy in hepatic metastasis: a preliminary investigation of reproducibility and diagnostic value.* J Magn Reson Imaging, 2014. **40**(2): p. 448-56.
47. Heijmen, L., et al., *Diffusion-weighted MR imaging in liver metastases of colorectal cancer: reproducibility and biological validation.* Eur Radiol, 2013. **23**(3): p. 748-56.
48. Miquel, M.E., et al., *In vitro and in vivo repeatability of abdominal diffusion-weighted MRI.* Br J Radiol, 2012. **85**(1019): p. 1507-12.
49. Gibbs, P., Pickles, M.D., L.W. Turnbull, *Repeatability of echo-planar-based diffusion measurements of the human prostate at 3T.* Magn Reson Imaging, 2007. **25**(10): p. 1423-9.
50. Jambor, I., et al., *Optimization of b-value distribution for biexponential diffusion-weighted MR imaging of normal prostate.* J Magn Reson Imaging, 2014. **39**(5): p. 1213-22.
51. Jambor, I., et al., *Evaluation of different mathematical models for diffusion-weighted imaging of normal prostate and prostate cancer using high b-values: a repeatability study.* Magn Reson Med, 2015. **73**(5): p. 1988-98.
52. Litjens, G.J., et al., *Interpatient variation in normal peripheral zone apparent diffusion coefficient: effect on the prediction of prostate cancer aggressiveness.* Radiology, 2012. **265**(1): p. 260-6.
53. Afaq, A., et al., *Clinical utility of diffusion-weighted magnetic resonance imaging in prostate cancer.* BJU Int, 2011. **108**(11): p. 1716-22.
54. Fedorov, A., et al., *Multiparametric MRI of the prostate: repeatability of volume and apparent diffusion coefficient quantification.* Invest Radiol, 2017. **(in press)**.
55. Winfield, J.M., et al., *Extracranial Soft-Tissue Tumors: Repeatability of Apparent Diffusion Coefficient Estimates from Diffusion-weighted MR Imaging.* Radiology, 2017: p. 161965.
56. Jackson, E.F., et al. *Acceptance Testing and Quality Assurance Procedures for Magnetic Resonance Imaging Facilities*
Report of MR Subcommittee Task Group I. 2010; Available from: http://www.aapm.org/pubs/reports/RPT_100.pdf.
57. Ellingson, B.M., et al., *Diffusion MRI quality control and functional diffusion map results in ACRIN 6677/RTOG 0625: a multicenter, randomized, phase II trial of bevacizumab and chemotherapy in recurrent glioblastoma.* Int J Oncol, 2015. **46**(5): p. 1883-92.
58. Shellock, F.G. and J.V. Crues, *MR procedures: biologic effects, safety, and patient care.* Radiology, 2004. **232**(3): p. 635-52.
59. Shellock, F.G. and A. Spinazzi, *MRI safety update 2008: part 2, screening patients for MRI.* AJR Am J Roentgenol, 2008. **191**(4): p. 1140-9.
60. Shellock, F.G. and A. Spinazzi, *MRI safety update 2008: part 1, MRI contrast agents and nephrogenic systemic fibrosis.* AJR Am J Roentgenol, 2008. **191**(4): p. 1129-39.
61. Shinbane, J.S., P.M. Colletti, and F.G. Shellock, *Magnetic resonance imaging in patients with cardiac pacemakers: era of "MR Conditional" designs.* J Cardiovasc Magn Reson, 2011. **13**: p. 63.
62. Ciet, P. and D.E. Litmanovich, *MR safety issues particular to women.* Magn Reson Imaging Clin N

Am, 2015. **23**(1): p. 59-67.
63. Enders, J., et al., *Reduction of claustrophobia during magnetic resonance imaging: methods and design of the "CLAUSTRO" randomized controlled trial.* BMC Med Imaging, 2011. **11**: p. 4.
64. Tee, L.M., et al., *Magnetic resonance imaging of the fetal brain.* Hong Kong Med J, 2016. **22**(3): p. 270-8.
65. Tsai, L.L., et al., *A Practical Guide to MR Imaging Safety: What Radiologists Need to Know.* Radiographics, 2015. **35**(6): p. 1722-37.
66. Calamante, F., et al., *MR system operator: recommended minimum requirements for performing MRI in human subjects in a research setting.* J Magn Reson Imaging, 2015. **41**(4): p. 899-902.
67. Ellingson, B.M., et al., *Consensus recommendations for a standardized Brain Tumor Imaging Protocol in clinical trials.* Neuro Oncol, 2015. **17**(9): p. 1188-98.
68. Chenevert, T.L., et al., *Diffusion coefficient measurement using a temperature-controlled fluid for quality control in multicenter studies.* J Magn Reson Imaging, 2011. **34**(4): p. 983-7.
69. Jerome, N.P., et al., *Development of a temperature-controlled phantom for magnetic resonance quality assurance of diffusion, dynamic, and relaxometry measurements.* Med Phys, 2016. **43**(6): p. 2998.
70. Malyarenko, D., et al., *Multi-system repeatability and reproducibility of apparent diffusion coefficient measurement using an ice-water phantom.* J Magn Reson Imaging, 2013. **37**(5): p. 1238-46.
71. Mulkern, R.V., et al., *Pediatric brain tumor consortium multisite assessment of apparent diffusion coefficient z-axis variation assessed with an ice-water phantom.* Acad Radiol, 2015. **22**(3): p. 363-9.
72. Malkyarenko, D.I. and T.L. Chenevert, *Practical estimate of gradient nonlinearity for implementation of apparent diffusion coefficient bias correction.* J Magn Reson Imaging, 2014. **40**(6): p. 1487-95.
73. Malyarenko, D.I., et al., *Demonstration of nonlinearity bias in the measurement of the apparent diffusion coefficient in multicenter trials.* Magn Reson Med, 2016. **75**(3): p. 1312-23.
74. Malyarenko, D.I., et al., *Correction of Gradient Nonlinearity Bias in Quantitative Diffusion Parameters of Renal Tissue with Intra Voxel Incoherent Motion.* Tomography, 2015. **1**(2): p. 145-151.
75. Malyarenko, D.I., B.D. Ross, and T.L. Chenevert, *Analysis and correction of gradient nonlinearity bias in apparent diffusion coefficient measurements.* Magn Reson Med, 2014. **71**(3): p. 1312-23.
76. Barth, M., et al., *Simultaneous multislice (SMS) imaging techniques.* Magn Reson Med, 2016. **75**(1): p. 63-81.
77. Eichner, C., et al., *Slice accelerated diffusion-weighted imaging at ultra-high field strength.* Magn Reson Med, 2014. **71**(4): p. 1518-25.
78. Obele, C.C., et al., *Simultaneous Multislice Accelerated Free-Breathing Diffusion-Weighted Imaging of the Liver at 3T.* Abdom Imaging, 2015. **40**(7): p. 2323-30.
79. Wu, X., et al., *Simultaneous multislice multiband parallel radiofrequency excitation with independent slice-specific transmit B1 homogenization.* Magn Reson Med, 2013. **70**(3): p. 630-8.
80. Sorensen, A.G., et al., *Hyperacute stroke: evaluation with combined multisection diffusion-weighted and hemodynamically weighted echo-planar MR imaging.* Radiology, 1996. **199**(2): p. 391-401.
81. van Gelderen, P., et al., *Water diffusion and acute stroke.* Magn Reson Med, 1994. **31**(2): p. 154-63.
82. Bastin, M.E., *Correction of eddy current-induced artefacts in diffusion tensor imaging using*

iterative cross-correlation. Magn Reson Imaging, 1999. **17**(7): p. 1011-24.
83. Le Bihan, D., et al., *Artifacts and pitfalls in diffusion MRI.* J Magn Reson Imaging, 2006. **24**(3): p. 478-88.
84. Mohammadi, S., et al., *Correcting eddy current and motion effects by affine whole-brain registrations: evaluation of three-dimensional distortions and comparison with slicewise correction.* Magn Reson Med, 2010. **64**(4): p. 1047-56.
85. Dyvorne, H.A., et al., *Diffusion-weighted imaging of the liver with multiple b values: effect of diffusion gradient polarity and breathing acquisition on image quality and intravoxel incoherent motion parameters--a pilot study.* Radiology, 2013. **266**(3): p. 920-9.
86. Kakite, S., et al., *Hepatocellular carcinoma: short-term reproducibility of apparent diffusion coefficient and intravoxel incoherent motion parameters at 3.0T.* J Magn Reson Imaging, 2015. **41**(1): p. 149-56.
87. LeBihan, D., *IVIM method measures diffusion and perfusion.* Diagn Imaging (San Franc), 1990. **12**(6): p. 133, 136.
88. Lee, Y., et al., *Intravoxel incoherent motion diffusion-weighted MR imaging of the liver: effect of triggering methods on regional variability and measurement repeatability of quantitative parameters.* Radiology, 2015. **274**(2): p. 405-15.
89. Takahara, T. and T.C. Kwee, *Low b-value diffusion-weighted imaging: emerging applications in the body.* J Magn Reson Imaging, 2012. **35**(6): p. 1266-73.
90. Yoon, J.H., et al., *Evaluation of hepatic fibrosis using intravoxel incoherent motion in diffusion-weighted liver MRI.* J Comput Assist Tomogr, 2014. **38**(1): p. 110-6.
91. Merisaari, H., et al., *Fitting methods for intravoxel incoherent motion imaging of prostate cancer on region of interest level: Repeatability and gleason score prediction.* Magn Reson Med, 2017. **77**(3): p. 1249-1264.
92. Basu, S., T. Fletcher, and R. Whitaker, *Rician noise removal in diffusion tensor MRI.* Med Image Comput Comput Assist Interv, 2006. **9**(Pt 1): p. 117-25.
93. Kristoffersen, A., *Optimal estimation of the diffusion coefficient from non-averaged and averaged noisy magnitude data.* J Magn Reson, 2007. **187**(2): p. 293-305.
94. Lui, D., et al., *Monte Carlo bias field correction in endorectal diffusion imaging.* IEEE Trans Biomed Eng, 2014. **61**(2): p. 368-80.
95. Chen, N.K. and A.M. Wyrwicz, *Removal of EPI Nyquist ghost artifacts with two-dimensional phase correction.* Magn Reson Med, 2004. **51**(6): p. 1247-53.
96. Guglielmo, F.F., et al., *Hepatic MR imaging techniques, optimization, and artifacts.* Magn Reson Imaging Clin N Am, 2014. **22**(3): p. 263-82.
97. Koh, D.M., et al., *Whole-body diffusion-weighted MRI: tips, tricks, and pitfalls.* AJR Am J Roentgenol, 2012. **199**(2): p. 252-62.
98. Kuhl, C.K., et al., *Sensitivity encoding for diffusion-weighted MR imaging at 3.0 T: intraindividual comparative study.* Radiology, 2005. **234**(2): p. 517-26.
99. Reese, T.G., et al., *Reduction of eddy-current-induced distortion in diffusion MRI using a twice-refocused spin echo.* Magn Reson Med, 2003. **49**(1): p. 177-82.
100. Bendel, P. and Y. Schiffenbauer, *A method for fat suppression in MRI based on diffusion-weighted imaging.* Phys Med Biol, 2010. **55**(22): p. N547-55.
101. Hansmann, J., D. Hernando, and S.B. Reeder, *Fat confounds the observed apparent diffusion coefficient in patients with hepatic steatosis.* Magn Reson Med, 2013. **69**(2): p. 545-52.
102. Hernando, D., et al., *Removal of olefinic fat chemical shift artifact in diffusion MRI.* Magn Reson Med, 2011. **65**(3): p. 692-701.

103. Nagy, Z. and N. Weiskopf, *Efficient fat suppression by slice-selection gradient reversal in twice-refocused diffusion encoding.* Magn Reson Med, 2008. **60**(5): p. 1256-60.
104. Sarlls, J.E., et al., *Robust fat suppression at 3T in high-resolution diffusion-weighted single-shot echo-planar imaging of human brain.* Magn Reson Med, 2011. **66**(6): p. 1658-65.
105. Kwee, T.C., et al., *Diffusion-weighted whole-body imaging with background body signal suppression (DWIBS): features and potential applications in oncology.* Eur Radiol, 2008. **18**(9): p. 1937-52.
106. Takahara, T., et al., *Diffusion-weighted magnetic resonance imaging of the liver using tracking only navigator echo: feasibility study.* Invest Radiol, 2010. **45**(2): p. 57-63.
107. Chenevert, T.L., et al., *Errors in Quantitative Image Analysis due to Platform-Dependent Image Scaling.* Transl Oncol, 2014. **7**(1): p. 65-71.
108. DICOM. *Parametric Map IOD Description*. Available from: http://dicom.nema.org/medical/dicom/current/output/chtml/part03/sect_A.75.html.
109. NEMA. *ADCmodelparameters*. Available from: ftp://medical.nema.org/medical/dicom/cp/cp1665_vp_ADCmodelparameters.pdf.
110. Delfino, J.G., *U.S. federal safety standards, guidelines and regulations for MRI systems: An overview.* Applied Radiology, 2015: p. 20-23.
111. Boss, M.A., et al. *Temperature-Controlled Isotropic Diffusion Phantom with Wide Range of Apparent Diffusion Coefficients for Multicenter Assessment of Scanner Repeatability and Reproducibility*. in *Proceeding of the International Society of Magnetic Resonance in Medicine*. 2014. Milan, Italy.
112. Sijbers, J. and A.J. den Dekker, *Maximum likelihood estimation of signal amplitude and noise variance from MR data.* Magn Reson Med, 2004. **51**(3): p. 586-94.
113. Friedman, L. and G.H. Glover, *Report on a multicenter fMRI quality assurance protocol.* J Magn Reson Imaging, 2006. **23**(6): p. 827-39.
114. Bammer, R., et al., *Analysis and generalized correction of the effect of spatial gradient field distortions in diffusion-weighted imaging.* Magn Reson Med, 2003. **50**(3): p. 560-9.

Appendices

Appendix A: Acknowledgements and Attributions

This document is proffered by the Radiological Society of North America [37], Diffusion-Weighted Imaging Task Force subgroup of the Perfusion Diffusion and Flow (PDF) Biomarker Committee. The PDF is composed of scientists, engineers, and clinicians representing academia, the imaging device manufacturers, image analysis software developers, image analysis laboratories, biopharmaceutical industry, government research organizations, professional societies, and regulatory agencies, among others. All work is classified as pre-competitive.

The following individuals have made critical contributions in the development of this Profile:

Rajpaul Attariwala
Daniel Barboriak
David Bennett
Ishtiaq Bercha
Michael Boss
Orest Boyko
Martin Büchert
Thomas Chenevert
Caroline Chung
Amita Shukla Dave
Andrey Fedorov
Clifton Fuller
Alexander Guimaraes
Marko Ivancevic
Edward Jackson
Ivan Jambor
John Kirsch
Daniel Krainak
Hendrik Laue
Jiachao Liang
Chen Lin
Mikko Määtta
Dariya Malyarenko
Elizabeth Mirowski
Bastien Moreau
Nancy Obuchowski
Estanislao Oubel
Savannah Partridge
Thorsten Persigehl
Mark Rosen
Mark Shiroishi
Rohit Sood
Daniel Sullivan
Ying Tang
Bachir Taouli
Aradhana Venkatesan
Ona Wu
Junqian Xu
Gudrun Zahlmann

We also acknowledge the extraordinary efforts by RSNA QIBA staff in making this Profile possible.

Appendix B: Background Information

QIBA Wiki:

http://qibawiki.rsna.org/index.php/Main_Page

QIBA Perfusion, Diffusion, and Flow Biomarker Committee Wiki:

http://qibawiki.rsna.org/index.php/Perfusion,_Diffusion_and_Flow-MRI_Biomarker_Ctte

DWI Literature Review:

http://qibawiki.rsna.org/index.php/DWI_Literature_Review

QIBAPhan Analysis Software (for ADC and summary statistics of isotropic diffusion phantom):

https://goo.gl/xjHc6G

QIBA DWI Digital Reference Object:

https://goo.gl/yYPG0W

Diffusion Phantom Preparation and Positioning:

http://qibawiki.rsna.org/index.php/Perfusion,_Diffusion_and_Flow-MRI_Biomarker_Ctte

DICOM MR Diffusion Macro:

http://dicom.nema.org/medical/dicom/current/output/chtml/part03/sect_C.8.13.5.9.html

Appendix C: Conventions and Definitions

Apparent Diffusion Coefficient (ADC): A quantitative imaging biomarker (typically in units mm^2/s or $\mu m^2/ms$) indicative of the mobility of water molecules. High ADC indicates free or less hindered mobility of water; low ADC indicates slow, restricted, or hindered mobility of water molecules.

***b*-value:** An indication of the strength of diffusion-weighting (typically in units of s/mm^2). It depends on a combination of gradient pulse duration, shape, strength, and the timing between diffusion gradient pulses.

DICOM: Digital Imaging and Communications in Medicine standard for distributing and viewing any kind of medical image regardless of the origin. A DWI DICOM header typically contains meta-data reflecting scan geometry and key acquisition parameters (e.g., *b*-value and gradient direction) required for subsequent generation of ADC maps and ROI statistics. A DWI DICOM macro assigns the required diffusion-specific attributes to public DICOM tags ([0018, 9087] & [0018, 9098]) which should be available independent of Vendor and scanner software version. Currently, vendors do not universally follow the DWI macro standard, storing *b*-value and direction metadata in private tags.

Diffusion Weighted Image (DWI): A type of MR image where tissue contrast is dependent on water mobility, diffusion gradient direction, concentration of water signal, and T_2 relaxation. On heavily diffusion-weighted images (i.e. high *b*-value), high signal indicates low water mobility, high proton concentration, and/or long T_2.

Isotropic (or trace) DWI: Directionally-independent diffusion-weighted images obtained as the composite (geometric average) of three orthogonal DWIs and used for ADC map derivation. Throughout this profile and assessment procedure, the term "DWI" refers to these directionally-independent images unless otherwise noted as a specific single-axis or directional DWI. Even in anisotropic media, directionally-independent (i.e. scalar) diffusion metrics are measurable using DWI combined from three-orthogonal diffusion gradient acquisitions.

Repeatability Coefficient (RC): Represents measurement precision where conditions of the

measurement procedure (scanner, acquisition parameters, slice locations, image reconstruction, operator, and analysis) are held constant over a "short interval".

Within-subject Coefficient of Variance (wCV): Is often reported for repeatability studies to assess repeatability in test–retest designs. Calculated as seen in the table below:

Steps for Calculating the wCV

1	Calculate the variance and mean for each of N subjects from their replicate measurements.
2	Calculate the wCV^2 for each of the N subjects by dividing their variance by their mean squared.
3	Take the mean of the wCV^2 over the N subjects.
4	Take the square root of the value in step 3 to get an estimate of the wCV.

Appendix D: Platform-Specific Acquisition Parameters for DWI Phantom Scans

For acquisition modalities, reconstruction software and software analysis tools, profile conformance requires meeting the activity specifications and assessment requirements above in Sections 2, 3 and 4.

This Appendix provides specific acquisition parameters, reconstruction parameters and analysis software parameters that are expected to achieve compatibility with profile requirements for technical assessment of MRI systems. Just using these parameters without meeting the requirements specified in the profile is not sufficient to achieve conformance. Conversely, it is possible to use different compatible parameters and still achieve conformance. System operation within provided conformance limits suggests the technical contribution to variance does not unduly alter wCV observed in biological measurements. Technical DWI performance of a given MRI system relative to peer systems can be assessed using the described standardized acquisition protocols designed for existing ice-water DWI phantoms. Platform-specific protocols were excerpted from the QIBA ice water-based DWI Phantom scan procedure for axial acquisitions. The full QIBA DWI Phantom scan procedure involves acquisitions for coronal, axial and sagittal planes as detailed in the QIBA DWI wiki.

Sites using MRI system models listed here are encouraged to consider using parameter settings provided in this Profile for both simplicity and consistency of periodic quantitative DWI QA procedures. Sites using models not listed here may be able to devise their own settings that result in data meeting the requirements of this Profile (at the minimum) or tighter requirements of specific clinical trial.

IMPORTANT: The presence of a product model/version in these tables does not imply it has demonstrated conformance with the QIBA Profile. Refer to the QIBA Conformance Statement for the product.

Table D.1 Model-specific Parameters for Acquisition Devices When Scanning DWI Phantoms

Acquisition Device	Settings Compatible with Conformance		
Philips	*Submitted by: University of Michigan, Department of Radiology*		
	Model / Version	Achieva / 5.1.7	Ingenia / 5.1.7
	Field Strength	1.5T	3T
	Receiver Coil	≥8ch head	≥ 15ch head
	Uniformity	CLEAR=yes; Body-Tuned=no	CLEAR = yes
	Slice Orientation	Transaxial	Transaxial
	FOV	220mm	220mm
	Acquisition Voxel Size	1.72x1.72x4mm	1.72x1.72x4mm
	Acquisition Matrix	128x126	128x128
	Recon Voxel Size	0.898x0.898x4mm	0.898x0.898x4mm
	Recon Matrix	256x256	256x256
	SENSE (parallel imaging)	Yes, factor=2	Yes, factor=2
	Fold-over Direction	AP	AP
	Fat-shift direction	P	P
	Foldover-sup / Oversampling	No	No
	Qty Slices	25	25
	Stacks and Packages	1	1
	Slice Thickness	4mm	4mm
	Slice gap (user-defined)	1mm	1mm
	Shim	Volume set to encompass phantom	Vol or PB-Vol to encompass phantom
	B1 shim	Not Applicable	Fixed
	Scan Mode	MS	MS
	Technique	SE	SE
	Acquisition Mode	Cartesian	Cartesian
	Fast Imaging Mode	EPI	EPI
	Shot Mode	Single-shot	Single-shot
	Echoes	1	1
	Partial Echo	No	No
	TE	Shortest (<110ms)	Shortest (<110ms)
	Flip Angle	90°	90°
	TR	10,000ms	10,000ms
	Halfscan factor	≥0.62	≥0.62
	Water-Fat shift (in phase dir)	Minimum (~11xAcqVoxel size)	Minimum (~24xAcqVoxel size)
	Fat suppression	No	No
	Diffusion Mode	DWI	DWI
	Direction	"M,P,S" (i.e. non-Overplus)	"M,P,S" (i.e. non-Overplus)
	b-values (user-defined)	0, 500, 900, 2000	0, 500, 900, 2000
	Average high *b*-values	No	No
	PNS Mode	High	High
	Gradient Mode	Maximum	Maximum
	NSA (averages)	1	1

	Images	M (magnitude)	M (magnitude)
	Preparation phases	Full for 1st scan; Auto for scan 2,3,4	Full for 1st scan; Auto for scan 2,3,4
	EPI 2D Phase Correction	No	No
	Save Raw Data	No	No
	Geometry Correction	Default	Default
	EPI Factor	67	67
	Bandwidth in Freq-direction	1534 Hz	1414 Hz
	Scan Duration	~2min/scan; 4scans for ~8min total	~2min/scan; 4scans for ~8min total

Acquisition Device	Settings Compatible with Conformance		
Siemens	*Submitted by: Siemens Healthcare*		
	Model / Version	Magnetom Aera / VD13	Magnetom Skyra/ VD13
	Field Strength	1.5T	3T
	Receiver Coil	HE1-4	HE1-4
	Slice Orientation	Transaxial	Transaxial
	FOV read and phase	220mm	220mm
	Base resolution	130	130
	Phase resolution	100%	100%
	Recon Voxel Size	0.8x0.8x4mm	0.8x0.8x4mm
	PAT Mode	GRAPPA, PE factor=2	GRAPPA, PE factor=2
	Phase enc Direction	A >> P	A >> P
	Ref lines PE	40	40
	Reference scan mode	Separate	Separate
	Qty Slices	25	25
	Phase oversampling	0%	0%
	Slice Thickness	4mm	4mm
	Distance Factor	25%	25%
	Shim mode	Standard	Standard
	Mode	2D	2D
	Multi-slice mode	Interleaved	Interleaved
	EPI factor	130	130
	Free Echo Spacing	Off	Off
	Echo spacing	0.77ms	0.94ms
	TE	98ms	104ms
	TR	10,000ms	10,000ms
	Fat suppression	No	No
	Diffusion Mode	Orthogonal	Orthogonal
	Diff. weightings	4	4
	b-value 1,2,3,4	0, 500, 900, 2000	0, 500, 900, 2000
	Diff. weighted images	On	On
	Trace weighted images	On	On
	Gradient Mode	Fast	Fast
	Averages	1	1
	Averaging mode	Long term	Long term
	Concatenations	1	1

	MTC	Off	Off
	Magn. preparation	None	None
	Filter	DistortionCorr(2D); PrescanNormalize	DistortionCorr(2D); PrescanNormalize
	Reconstruction	Magnitude	Magnitude
	Bandwidth	1538 Hz/Px	1424 Hz/Px
	RF pulse type	Normal	Normal
	Scan Duration	~2min/scan; 4scans for ~8min total	~2min/scan; 4scans for ~8min total

Acquisition Device	Settings Compatible with Conformance		
General Electric	*Submitted by: Memorial Sloan Kettering Cancer Center; and GE Healthcare*		
	Model / Version	Optima MR 450 / DV23.1	Discovery MR 750 / DV23.1
	Field Strength	1.5T	3T
	Receiver Coil	8HRBrain	8HRBrain
	Slice Orientation	Transaxial	Transaxial
	FOV	22cm	22cm
	Phase FOV	100%	100%
	Acquisition matrix	128x128	128x128
	Acq voxel size	1.72x1.72x4mm	1.72x1.72x4mm
	Recon voxel size	0.98x0.98x4mm	0.98x0.98x4mm
	ASSET Acceleration, Phase	2	2
	Freq enc Direction	R/L	R/L
	Qty Slices	25	25
	Slice Thickness	4mm	4mm
	Slice spacing	1mm	1mm
	Shim	Auto	Auto
	Imaging Options	2D, spin-echo, EPI, DIFF	2D, spin-echo, EPI, DIFF
	Num Shots	1	1
	Dual Spin Echo	No	No
	TE	Min Full (~123ms)	Min Full (~104ms)
	TR	10,000ms	10,000ms
	Fat suppression	No	No
	Diffusion Direction	ALL	ALL
	b-value	0, 500, 900, 2000	0, 500, 900, 2000
	Phase Correct	On	On
	dB/dt control mode	1st	1st
	NEX	1	1
	Bandwidth	Default (250kHz)	Default (250kHz)
	3D Geometry correction	No	No
	Scan Duration	~2min/scan; 4scans for ~8min total	~2min/scan; 4scans for ~8min total

Appendix E: Technical Assessment Procedures

Procedures below are for basic assessment of MRI equipment in conformance to the quantitative DWI Profile. Conformance limits for performance metrics are suggested to ensure that technical measurement errors related to the MRI system do not unduly contribute to measurement variance.

E.1. ASSESSMENT PROCEDURE: ADC QUALITIES AT/NEAR ISOCENTER

This activity describes criteria that are necessary for an MRI system to meet the quantitative DWI Profile Claims.

E.1.1 Discussion

To assess an MRI system for ADC measurement bias and precision, a phantom containing media having known diffusion properties is required. Water maintained at 0°C is widely used as a known standard with diffusion coefficient = 1.10×10^{-3} mm^2/s, and is the basis for ice water-based DWI phantoms [68-70]. This assessment procedure requires the assessor have access to an ice water DWI phantom, such as the QIBA DWI phantom [111] or alternative that contains a measurement sample of water (≥30 mL volume) located at isocenter surrounded by an ice water bath [68-70]. The assessor must allow sufficient time for the sample to achieve thermal equilibrium (≥1 hour) and the phantom must contain an adequate volume of ice to surround the measurement sample over the entire MRI exam period. Details for preparation and use of the QIBA DWI phantom are available in the QIBA DWI wiki. This assessment procedure requires the assessor follow the core DWI scan parameters defined in Appendix D, Table 2, which involves acquisition of diffusion weighted images of the phantom at nominal *b*-values = 0, 500, 900, 2000 s/mm^2.

Typically, MRI systems exhibit best performance at or near isocenter where ADC bias reflects overall calibration of gradient amplitude and DWI sequence timing. For this procedure, proximity to isocenter is to be determined by location of the center of an ROI used to assess ADC. Spatial coordinates of the ROI-center are often available using the scanner's electronic caliper read-out of ROI-center coordinates in the patient-based frame of reference defined by assessor's "Patient Landmark" location. Note, the patient-based frame and magnet-based frame (true isocenter) may not be synonymous, and displacement between the two may vary from scan series to scan series. To maintain minimal offset between patient-based and magnet-based frames, the assessor shall define the "Patient Landmark" on the center of the phantom then keep the prescription of slices used for quantitative assessment centered on Superior/Inferior=0 mm (for cylindrical bore magnets). For this procedure, an ROI having center coordinates [*RL, AP, SI*] is "at isocenter" when $\sqrt{RL^2 + AP^2 + SI^2} \leq 4\ cm$, and the maximum diameter of the ROI ≤ 2 cm. A minimum ROI diameter of ~1cm will provide sufficient number of pixels (>80) for adequate sampling of phantom ADC heterogeneity for reliable estimate of within ROI statistics (standard deviation and mean). For uniform analysis, "QibaPhanR1.4" software provided through the QIDW can be used to generate the relevant ADC ROI assessment metrics (bias, precision, repeatability and SNR) for QIBA DWI phantom, as described below.

The QIBA DWI phantom, and other water-based phantoms are isotropic so measured diffusion coefficient ***should*** be independent of applied diffusion gradient direction. Throughout this profile and assessment procedure, "DWI" will refer to the composite of three orthogonal DWIs as the trace DWI.

Two or more diffusion weightings are required to calculate ADC, and full ADC maps are generated on a pixel-by-pixel basis (though low SNR may bias these pixel-by-pixel ADC maps) using the mono-exponential model:

$$ADC_{bmin,b} = \frac{1}{(b-bmin)} \ln\left[\frac{S_{bmin}}{S_b}\right], \qquad \text{EQ(1)}$$

where S represents the diffusion weighted image intensity and subscripts refer to *b*-value. For this assessment procedure, if only two b-values are used, they must include the nominal minimum *b*-value in the calculation, typically *b*=0. If all b-values are used in the ADC calculation, a mono-exponential signal decay versus *b*-value model fit (e.g., least-squares) must be used. To achieve adequate diffusion contrast

for ADC estimation via EQ(1), $(b - b_{min})$ shall be $\geq$ 400 s/mm^2.

The estimate of MRI system ADC bias in measurement of 0°C water (DC_{true} = 1.1x10^{-3} mm^2/s [68]) at isocenter shall be calculated as:

$$ADC\ bias\ estimate = \mu - DC_{true};\ or\ \%bias = \frac{100\%\ (\mu - DC_{true})}{DC_{true}},\qquad \text{EQ(2)}$$

where μ is the ROI mean of the ADC map at isocenter and the ROI contains 80-150 pixels. Assuming the pixel values follow a normal distribution, the 95% confidence interval (CI) for this bias estimate is,

$$ADC\ bias\ estimate\ \pm 1.96\ \frac{\sigma}{\sqrt{N}},\qquad \text{EQ(3)}$$

where σ is the standard deviation of ADC pixel values in the ROI containing *N* pixels.

The standard deviation of ADC pixel values within an isocenter ROI is one indicator of random measurement error (precision) in ADC maps expressed as a percentage relative to the ROI mean (%CV) as:

$$ADC\ error\ estimate = 100\% \cdot \frac{\sigma}{\mu}\qquad \text{EQ(4)}$$

Similar to ADC bias estimate, this procedure typically uses an ROI of ~1 cm^2 (>80 pixels) on a water sample at 0 °C (e.g. center tube of QIBA DWI phantom) at isocenter, and follow the QIBA DWI phantom scan protocol to estimate ADC error.

The established QIBA DWI phantom scan protocol is to acquire four DWI scans (each ~2 minutes) in immediate succession holding acquisition conditions constant. This procedure serves multiple aims: (1) inspect for monotonic trend in ADC vs time suggesting the phantom was not at thermal equilibrium; (2) inspect for artifact or drift suggesting system instability; (3) allow for estimation of voxel signal-to-noise ratio (SNR); and (4) provide an estimate of short-term (intra-exam) repeatability [68, 70]. Repeated scanning of the phantom over multiple days/weeks/months more closely resembles serial scanning of patients in longitudinal studies. Regardless of interval over which repeated measurements are performed, assuming normally distributed measures, the Repeatability Coefficient (RC) and "within-subject" Coefficient of Variation as a percentage (wCV) are calculated as [30, 35, 36]:

$$RC = 2.77 \cdot \sigma_w;\quad wCV = 100\%\ \frac{\sigma_w}{\mu},\qquad \text{EQ(5)}$$

where σ_w^2 is the within-subject (phantom) parameter variance and μ is the parameter mean. The average of repeated ROI means at isocenter and square root of variance of these means may be used in EQ(5) to estimate *RC* and *wCV* as a metric of system technical performance. Please note, phantom-based *RC* and *wCV* derived here are under relatively ideal conditions and should not be taken as representative of repeatability achieved in human DWI/ADC studies that involve more sources of variability.

E.1.2 Specification

Parameter	Actor	Requirement
ADC bias at/near isocenter		|ADC bias| $\leq$ 0.04x10^{-3} mm^2/s, or $\leq$ 3.6% per instructions above
ADC error at/near		ADC random error $\leq$ 2% per instructions above

isocenter	Acquisition Device / Physicist / Scientist	
Short-term (intra-exam) ADC repeatability at/near isocenter		RC $\leq$ 1.5x10^{-5} mm^2/s and *wCV* $\leq$ 0.5% per instructions above
Long-term (multi-day) ADC repeatability at/near isocenter		RC $\leq$ 6.5x10^{-5} mm^2/s and wCV $\leq$ 2.2% per instructions above

E.2. Assessment Procedure: DWI Signal to Noise

This activity describes criteria that are necessary for an MRI system to meet the Profile Claim. This procedure can be used by a vendor or an imaging site to estimate relative signal-to-noise ratio (SNR) of an MRI system in the context of DWI and parametric ADC maps (both for phantom and subjects).

E.2.1 Discussion

Signal-to-noise ratio of any MR image is heavily dependent on acquisition conditions so while SNR is informative of system performance, its assessment by the suggested procedure is not an absolute system performance metric. Determination of SNR by this procedure serves two aims: (1) provide a relative system performance metric; and (2) confirm SNR was adequate to measure ADC bias without incremental bias due to low SNR.

This procedure is used to assess SNR at the acquisition voxel level. Common filtering, interpolation and reconstruction algorithms lead to correlated noise in neighboring DWI pixels. Therefore, the described procedure relies on analysis that yields a noise estimate averaged over an ROI to mitigate effect of correlated noise.

Signal estimated as the mean pixel intensity value over an ROI is straightforward; however, DWI noise estimation is more difficult. Using standard deviation of pixel values in signal-free background (i.e. air) as noise estimate is unreliable due to commonly-used parallel imaging reconstruction, coil-sensitivity equalization routines and Rician bias of "magnitude" signals [92-94, 112]. Instead for this procedure, noise will be estimated by the temporal change in pixel values measured over multiple scans. The QIBA DWI phantom scan protocol requires four scans repeated in immediate succession holding all acquisition conditions constant. Images containing the measurement ROI over these four dynamics shall be visually inspected for conspicuous (multi-pixel) spatial shift, distortion, or artifact in any of the dynamics. Assuming none, random noise is considered to be the main contributor to scan-to-scan differences. To assess noise by this procedure, software (similar to "QibaPhanR1.4") must be available to combine dynamic images and calculate the temporal standard deviation of each pixel (i.e. over the "n" dynamic scans). An image comprised of the temporal standard deviation of pixel values shall be referred to as the "temporal noise image". An image comprised of the temporal mean of pixel values shall be referred to as the "signal image". Note, an image comprised of the pixel-by-pixel division of the signal image by the temporal noise image is referred to as the "signal-to-fluctuation-noise-ratio image" [113], but this should not be used to estimate SNR. Instead, the calculation estimates noise as spatial mean within an ROI of

temporal noise image and corresponding signal as a spatial ROI mean of the temporal average signal image [112]:

$$SNR_{nDyn} = \frac{Spatial\ mean\ pixel\ value\ \ on\ Signal\ Image}{Spatial\ mean\ pixel\ value\ on\ Temporal\ Noise\ Image} \quad \text{EQ(6)}$$

The 95% confidence interval for this SNR estimate is $\pm 1.96\ \frac{\sigma_{SNR}}{\sqrt{N}}$,

where $\sigma_{SNR} = SNR_{nDyn}\sqrt{sCV^2 + nCV^2}$ is the "error propagation" estimate of standard deviation of SNR pixel values in an ROI containing *N* pixels with spatial coefficients of variance, sCV and nCV, for the temporal average signal image and temporal standard-deviation noise image, respectively.

An alternative procedure to estimate SNR from an even quantity of dynamic scans is to first sum all odd-numbered dynamics called "sumODD image" and sum all even-numbered dynamics called "sumEVEN image", then create their difference called "DIFF image" = sumODD – sumEVEN. Using these, an estimate of SNR within an ROI from n-dynamic scans acquired in immediate succession holding conditions fixed shall be calculated as [113]:

$$altSNR_{nDyn} = \sqrt{n}\ \frac{Spatial\ mean\ pixel\ value\ on\ Signal\ Image}{Spatial\ standard\ deviation\ pixel\ value\ on\ DIFF\ Image}\ . \quad \text{EQ(7)}$$

EQ(7) shall be used when only two dynamic scans (n=2) are available.

For conditions defined in this assessment procedure (i.e. 4 dynamics and 80-100 pixel ROIs) equation EQ(6) tends to overestimate SNR slightly although has tighter confidence interval relative to equation EQ(7). The choice of which equation to use may depend on capabilities of the analysis software. SNR analysis via equations EQ(6) and/or EQ(7) may be performed on source DWI images, as well as on derived ADC maps.

In situations where two or more dynamic series are not available, the "noise" level may be crudely estimated (i.e. still subject to Rician bias and background regularization) by the standard deviation in signal-free background or by the standard deviation within the ROI defined on uniform signal-producing area. Prior to defining the background ROI, the assessor must inspect the images with a tight window/level and strive to select a background region that contains uniform random noise while avoiding signal gradients, structured noise (e.g. ghosts) or severely modulated zones (often masked to "zero"). While considered unreliable for reasons stated above, the equation to estimate SNR of an ROI in signal-producing region relative to background region is:

$$SNR_{vs\ bkgnd} = \frac{Spatial\ mean\ pixel\ value\ on\ Signal\ Image}{Spatial\ standard\ deviation\ pixel\ value\ in\ background\ ROI}\ . \quad \text{EQ(8)}$$

Since performed on magnitude images, this procedure under-estimates noise thus over-estimates SNR. This Rician bias may be predicted using DWI DRO and could be appropriately factored into further analysis of ADC statistics [92, 93, 112].

At a minimum, the assessment procedure outlined in EQ(6) and EQ(7) shall be performed on the *b*=0 diffusion weighted image. Low SNR conditions can introduce bias in ADC measurement (see Figure E.1). To be conformant with this profile and avoid introduction of bias due to low SNR conditions, an MRI system shall have SNR $\geq$ 50±5 for the *b*=0 image in an ROI of 1 cm diameter (80-100 pixels). This SNR will allow measurement of mono-exponential diffusion media having diffusion coefficients $\leq$ 1.1x10^{-3} mm^2/s (e.g. water at 0 °C) using *b*-values $\leq$ 2000s/mm^2 and avoid incremental bias due to noise. SNR limits for different ADC and *b*-value ranges relevant for clinical trials can be assessed using DWI DRO provided through QIDW (Figure E.1).

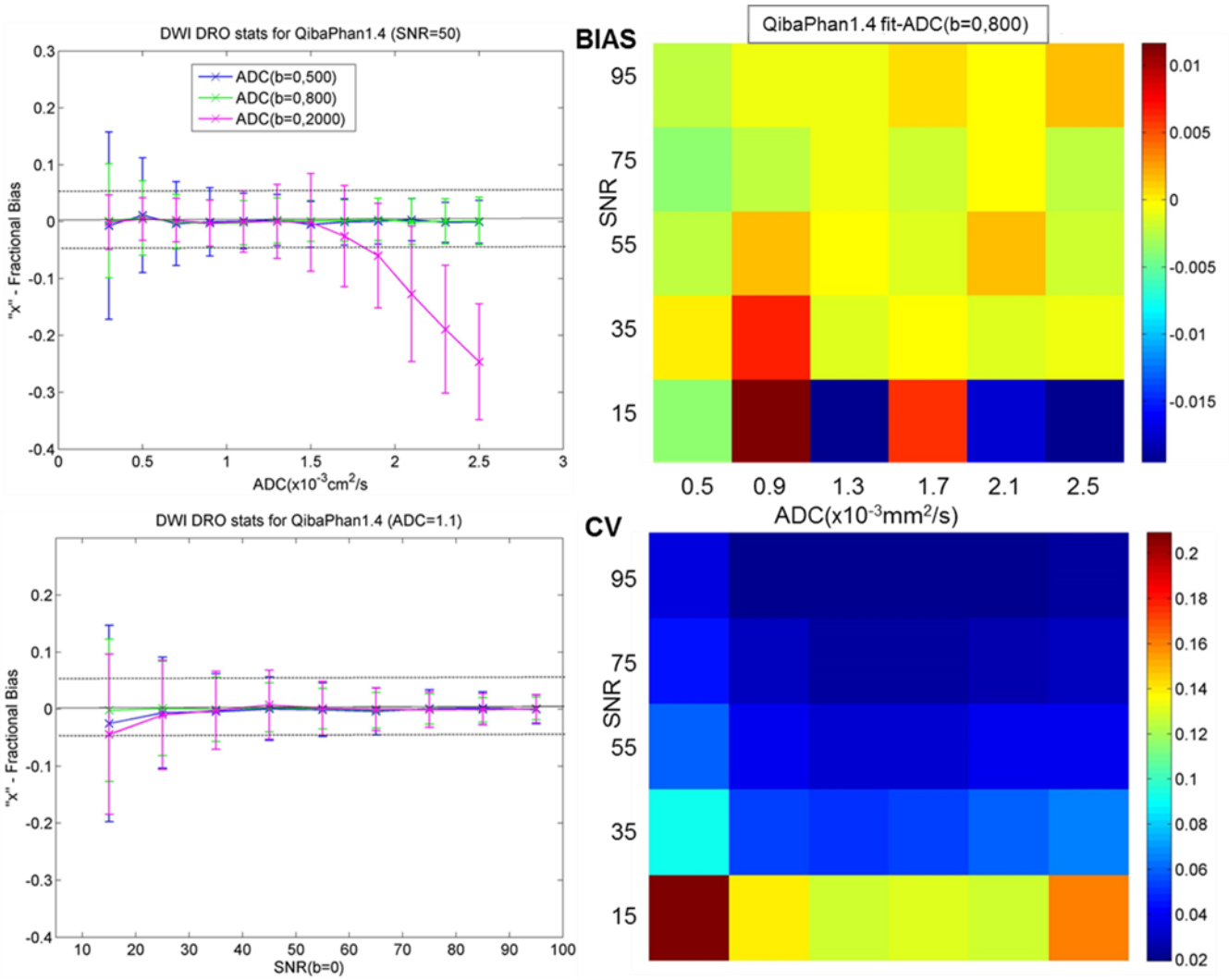

Figure E.1: Examples of fractional-bias and CV metrics for DWI-DRO ADC maps generated using QibaPhan1.4 SW. Left panes show fractional ADC bias and SD (error-bars) as a function of true (i.e., DRO input) ADC (top: at SNR=50) and SNR (bottom: at ADC=1.1 x10^{-3}mm^2/s) for three b-values (color-coded in legend). The dotted horizontal lines mark ±5% deviation to guide optimal DWI parameter ranges for ADC, SNR, b-value. Mean bias appears to be dependent on ADC and b-value and independent of SNR, while bias SD closely follows CV-trend and mostly SNR-dependent. Right panes show the SNR/ADC maps for mean bias and CV metrics at b-value=800 (typical of liver DWI protocol), indicating that the fit-ADC bias error (mean +/- SD) falls within +/-5% for SNR>50 in liver ADC range (0.7-1.7)x10^{-3}mm^2/s.

E.2.2 Specification

Parameter	Actor	Requirement
DWI *b*=0 SNR	Acquisition Device / Image Analyst / Scientist	SNR (*b*=0) ≥ 50±5 per instructions above.

E.3. Assessment Procedure: ADC *b*-value dependence

This activity describes criteria that are necessary for an MRI system to meet the Profile Claims. This procedure can be used to document artefactual *b*-value dependence in ADC measurements.

E.3.1 Discussion

The QIBA DWI phantom and other ice water phantoms ***should*** exhibit mono-exponential signal decay with increasing *b*-value. Any apparent change in measured ADC with choice of *b*-value suggests one or combination of the following: (1) output gradient amplitude is not linear with input demand; (2) background gradients that have substantial but variable contribution to the actual *b*-value; (3) spurious signal in $b \approx 0$ DWI that is eliminated at moderately low *b*-values (e.g. $b \geq 50$ s/mm^2); and (4) inadequate SNR at high *b*-values. To assess whether an MRI system exhibits artefactual b-value dependence in ADC measurement, the assessor shall compare ADC values measured at isocenter on an ice water phantom as a function of *b*-value pairs described in equation 1. The lowest *b*-value (typically $b_{min} = 0$) must be included in each *b*-value pair. The assessor shall calculate *b*-value dependence as:

$$ADC\ bvalue\ dependence = 100\% \left\| \frac{(ADC_{bmin,b2} - ADC_{bmin,b1})}{ADC_{bmin,b1}} \right\|, \qquad \text{EQ(9)}$$

where $b_2 \neq b_1$. Note, adequate diffusion contrast is required for ADC estimation via EQ(1), therefore both $(b_1 - b_{min})$ and $(b_2 - b_{min})$ shall be $\geq$ 400 s/mm^2.

E.3.2 Specification

Parameter	Actor	Requirement
ADC *b*-value dependence	Acquisition Device / Physicist / Scientist	< 2% per instructions above.

E.4. Assessment Procedure: ADC spatial dependence

This activity describes criteria that are necessary for an MRI system to meet the Profile Claim. This procedure can be used to document artefactual spatial non-uniformity of ADC measurements.

E.4.1 Discussion

All ADC calculations described above utilize nominal *b*-values entered by the assessor during DWI acquisition and retained in DICOM headers. In turn, *b*-value selection determines amplitude and timing of diffusion-encoding gradient pulses within the diffusion sequence. Due to current physical constraints of gradient designs, gradient strength is not spatially uniform throughout the imaged volume. The greatest contributor to non-uniformity in ADC maps is gradient nonlinearity (GNL), although other sources such as uniformity of the main magnetic field can also contribute to spatial ADC bias at off-center locations [72-75, 114]. Regardless of source, the maximum level of allowable ADC spatial non-uniformity of an MRI system depends on scale of the imaging volume for the specific clinical application. For example, DWI studies dedicated to the prostate or brain lesions could benefit from relatively minimal expected GNL spatial bias when the imaging prescription requires the lesion be located near superior/inferior = 0mm;

whereas bilateral breast or unilateral off-center liver DWI will likely experience greater GNL bias. For MRI system performance assessment, a DWI phantom should be selected that reasonably spans the imaging volume of the associated clinical application and that preferably fits in the same application-specific receiver coil. By its physical nature (determined by gradient coil design), spatial non-uniformity GNL bias is expected to be independent of *b*-value and ADC range. Thus, assessment of this bias for phantom is a reasonable estimate for bias in patient scans in clinical trials. In the context of clinical trial, GNL non-uniformity bias is expected to increase both the ROI ADC error (i.e. in ROI mean and ADC histogram width, and increasing wCV), and the variability among systems.

The assessor shall use a DWI phantom having known diffusion coefficient, such as the QIBA DWI phantom or other suitable ice water-based phantom, follow established phantom preparation instructions, and acquire DWI using a protocol matched to the associated application. Using EQ(2), ADC bias shall be assessed in multiple ROIs of at least 80 pixels each that reasonably sample spatial offset(s) from magnet isocenter anticipated for the specific clinical application. Maximum allowed bias for a system compliant to this profile will increase with maximum allowed offset from isocenter. For MRI systems conformant to this profile, maximum allowed bias for select spatial offsets are illustrated in specifications below.

E.4.2 Specification

Parameter	**Actor**	**Requirement**
Maximum |bias| with offset from isocenter:	Acquisition Device / Physicist / Scientist	
within 4 cm in any direction		< 4%
Right or Left < 10 cm with A/P and S/I <4 cm		< 10%
Anterior or Posterior < 10 cm with R/L and S/I <4 cm		< 10%
Superior or Inferior < 5 cm with R/L and A/P <4 cm		< 10%

Note that with other performance assessment metrics conformant to the Profile, the listed acceptable ranges for ADC non-uniformity bias could be the major source of the technical measurement error (both for wCV and mean ADC bias) limiting ADC confidence intervals.